HHS Public Access

Author manuscript

Gene. Author manuscript; available in PMC 2019 July 20.

Published in final edited form as:

Gene. 2018 July 20; 664: 152–167. doi:10.1016/j.gene.2018.04.048.

MYH9: STRUCTURE, FUNCTIONS AND ROLE OF NON-MUSCLE MYOSIN IIA IN HUMAN DISEASE

Alessandro Pecci[a], **Xuefei Ma**[b], **Anna Savoia**[c,d], and **Robert S. Adelstein**[b]

[a]Department of Internal Medicine, IRCCS Policlinico San Matteo Foundation and University of Pavia, Piazzale Golgi, 27100 Pavia, Italy

[b]Laboratory of Molecular Cardiology, National Heart, Lung, and Blood Institute, National Institutes of Health, Bldg. 10 Room 6C-103B, 10 Center Drive, Bethesda, MD 20892-1583, USA

[c]Department of Medical Sciences, University of Trieste, via Dell'Istria, 65/1, I-34137 Trieste, Italy

[d]IRCCS Burlo Garofolo, via Dell'Istria, 65/1, I-34137, Trieste, Italy

Abstract

The *MYH9* gene encodes the heavy chain of non-muscle myosin IIA, a widely expressed cytoplasmic myosin that participates in a variety of processes requiring the generation of intracellular chemomechanical force and translocation of the actin cytoskeleton. Non-muscle myosin IIA functions are regulated by phosphorylation of its 20kDa light chain, of the heavy chain, and by interactions with other proteins. Variants of *MYH9* cause an autosomal-dominant disorder, termed *MYH9*-related disease, and may be involved in other conditions, such as chronic kidney disease, non-syndromic deafness, and cancer. This review discusses the structure of the *MYH9* gene and its protein, as well as the regulation and physiologic functions of non-muscle myosin IIA with particular reference to embryonic development. Moreover, the review focuses on current knowledge about the role of *MYH9* variants in human disease.

Keywords

MYH9 gene; non-muscle myosin; class II myosin; *MYH9*-related disease; cell-cell adhesion; mouse models; actin-myosin cytoskeleton; inherited thrombocytopenia; kidney disease; deafness; tumor suppressor

Corresponding author: Alessandro Pecci, Department of Internal Medicine, IRCCS Policlinico San Matteo Foundation and University of Pavia, Piazzale Golgi, 27100 Pavia, Italy. Tel.: +39.0382.5021358. Fax: +39.0382.526223. alessandro.pecci@unipv.it.

CONFLICTS OF INTEREST

The authors declare no conflicts of interest.

AUTHOR CONTRIBUTIONS

The authors contributed equally in writing this paper.

INTRODUCTION

The *MYH9* gene encodes the heavy chain of non-muscle myosin of class II, isoform A (NM IIA). Myosins constitute a superfamily of motor proteins that bind to actin and produce mechanical force through magnesium-dependent hydrolysis of ATP. The members of this family are grouped into more than 30 classes that have variable distribution and play distinct functions (Foth et al., 2006; Odronitz and Kollmar, 2007; Sebé-Pedrós et al., 2014). Class II includes muscle myosins, which generate the contraction of striated and smooth muscles. This class also includes non-muscle myosins, which are expressed in all eukaryotic cells where they participate in a variety of processes requiring the production of force and translocation of the actin cytoskeleton, such as cytokinesis, cell migration, polarization, and adhesion, maintenance of cell shape, and signal transduction. Mammalian cells express three isoforms of class II non-muscle myosin, NM IIA, IIB, and IIC, which differ in their heavy chains, which are encoded by three distinct genes, *MYH9*, *MYH10*, and *MYH14*, respectively (Marigo et al., 2004). This review will focus on the structure, regulation, and physiologic functions of *MYH9* and NM IIA, and will then discuss the current knowledge on the role of variants of *MYH9* in human disease. For general reviews on class II non-muscle myosins, see (Dulyaninova and Bresnick, 2013; Heissler and Manstein, 2013; Heissler and Sellers, 2016; Ma and Adelstein, 2014; Vicente-Manzanares et al., 2009).

STRUCTURES OF THE *MYH9* GENE AND PROTEIN

MYH9 is a large gene localized on chromosome 22q12.3, spanning more than 106 kbp and composed of 41 exons. The open reading frame, spread from exon 2 to exon 41, encodes a protein of 1,960 amino acids, the non-muscle myosin heavy chain IIA (NMHC IIA) (Figure 1A). The analysis of the basal promoter region indicates that *MYH9* is a typical housekeeping gene having no TATA box but high GC content, with multiple GC boxes. Two enhancer regions have also been characterized 23–150 kb downstream of the promoter in intron 1.

Similar to all myosins of class II, NM IIA is a hexameric molecule consisting of a homodimer of heavy chains (230 kDa), two regulatory light chains (20 KDa) controlling the myosin activity, and two essential light chains (17 kDa), which stabilize the heavy chain structure (Figure 1B). Each heavy chain recapitulates the general structure of class II myosins and comprises two anatomically distinct domains: the N-terminal head domain, which consists of the globular motor domain and the neck domain, and the C-terminal tail domain (Eddinger and Meer, 2007). The motor domain is responsible for actin binding and generation of force through MgATPase activity. The three-dimensional structure of the motor domain consists of four subdomains connected by flexible linkers: the N-terminal SH3-like motif, the upper and the lower 50kDa subdomains, and the converter region (Sellers, 2000). The neck acts as a lever arm that amplifies the movement produced by conformational changes of the motor domain and serves as the binding site for the light chains through two IQ motifs. The tail domain is responsible for both dimerization of the heavy chains and formation of NM IIA functional filaments. In fact, two heavy chains dimerize through the tail domain forming a long alpha-helical coiled-coil rod constituted of typical heptad repeats. In the unfolded active form of NM IIA (6S, see below), dimers self-

associate through the coiled-coil region to form bipolar filaments, which bind to actin through the protruding head domains and move actin filaments in an anti-parallel manner (Figure 2). The tail domain ends at the C-terminus with a 34-residue non-helical tailpiece, which contains a phosphorylation site (Serine 1943) with regulatory functions, as detailed below. Of the *MYH9* coding exons, the region from exon 2 to exon 19 encodes the motor domain, exon 20 the neck, and exons 21 to 40 the coiled-coil of the NMHC IIA. The 34 C-terminal amino acids of the non-helical tailpiece are encoded by exon 41.

MYH9 is a well-conserved gene through evolution from fungi to mammals. Its mouse ortholog (*Myh9*) is localized in a syntenic region on chromosome 15 (D'Apolito et al., 2002). Spanning more than 81 kbp, *Myh9* has the same genomic organization as that of the human gene and encodes a protein of the same length, with 97.1% amino acid identity with the MYH9 protein, suggesting that the mouse is a good model to study the role of *MYH9* and the pathogenetic mechanisms responsible for human diseases due to *MYH9* mutations.

Other non-muscle myosins of class II

The *MYH10* gene is located on chromosomes 17p13.1 and encodes the heavy chain of NM IIB, which is a protein of 1,976 amino acids sharing 77.7% identity and 88.5% similarity with NMHC IIA. On chromosome 19q13.33 is *MYH14* encoding the heavy chain of NM IIC, a protein 1,995 amino acids long with 63.4% identity and 79.7% similarity with NMHC IIA. Within the three heavy chains similarity is 90–92% among the motor domains and 75–77% among the tail domains (Marigo et al., 2004). There are isoforms of MYH10 and MYH14 due to insertions of one or two in-frame alternative exons. Considering that *MYH9*, *MYH10* and *MYH14* have the same genomic structure with the first exon being untranslated and 40 coding exons, they are likely to have been generated from duplications of a common ancestral gene and to have evolved to play different functions, though their high homology allows the NMs II to have partially redundant biological properties, as discussed below.

REGULATION OF THE STRUCTURE AND FUNCTION OF NM IIA

NM IIA is the most widely distributed of the three NM II isoforms. It is present in a large variety of cells and is expressed during early embryonic development. It accounts for 80% of total NM II in the protein extract prepared from cultured mouse embryonic stem cells (mESCs), where no NM IIC is detected (Ma et al., 2010). It is the sole NM II detected in the developing visceral endoderm in mice (Conti et al., 2004) and though it is present in the early developing cardiac outflow tract, it is entirely absent from mature cardiac myocytes (Ma and Adelstein, 2012). NM IIA is detected in all other cells examined in developing mouse embryos by immunostaining of tissue sections. As seen in Figure 3, NM IIA is present in the early embryo and surrounding, supporting structures (A), in the developing embryonic organs (B) and in the vasculature of the developing brain (B,C). By E16.5 it is absent from the cardiac myocytes in the heart but is present in the non-muscle cells and vasculature (D). At this embryonic age it is present throughout the lungs (E) and enriched in the intestinal cells (F). Mature platelets and lymphocytes contain only NM IIA. Moreover, in a number of cell lines and adult tissues the percent of NM IIA is significantly greater than the other two isoforms (Ma et al., 2010; Golomb et al., 2004). Cells, including cardiac

myocytes and smooth muscle cells, when placed into culture with serum initiate or increase the expression of NM IIA (Takeda et al, 2003; Kawamoto and Adelstein, 1991).

NM IIA in Visceral Endoderm Cell-Cell Adhesion

Expression of NM IIA is essential for the formation of a functional visceral endoderm during early embryonic development of mice (Conti et al., 2004). Mice genetically ablated for NM IIA die by E6.5 with a major defect in visceral endoderm formation. These knock out (*Myh9* −/−) mice fail to form E-cadherin mediated adherent cell-cell junctions between the endoderm cells. Instead of forming a normal polarized columnar layer, the NM IIA ablated visceral endoderm is disorganized and fails to support embryo development through gastrulation. The visceral endoderm of these mice also shows marked evidence for defects in cytokinesis, including multinucleation and malformed nuclei. Interestingly, the role of NM IIA in the development of a functional visceral endoderm can be substituted for by either NM IIB (Wang et al., 2010) or NM IIC1 (the most abundant alternatively spliced isoform of NM IIC). Mice expressing NM IIB or IIC1 in place of NM IIA were generated by genetically ablating and replacing NMHC IIA with cDNA encoding NMHC IIB or NMHC IIC1, thereby expressing NMHC IIB or IIC1 under control of the endogenous NMHC IIA promoter. These mice develop a normal visceral endoderm and survive beyond organogenesis. E-cadherin localization is restored to the normal cell-cell adhesion complex together with NM IIB (or NM IIC1) and no defect in cytokinesis is observed in these mice. Moreover, the function of NM IIA in maintaining cell-cell adhesion in the visceral endoderm does not require full NM IIA motor activity. This was demonstrated by substituting arginine 702 with cysteine (p.R702C) in NMHC IIA (Zhang et al., 2012). This point mutation results in a compromised myosin MgATPase activity but the mutant myosin can still support functional visceral endoderm formation in mice, despite causing other severe abnormalities such as defects in placenta formation.

Embryonic stem cells also require NM II to maintain E-cadherin mediated adherent cell-cell junctions. Unlike the visceral endoderm where no other NM II isoforms (IIB and IIC) are expressed, mESCs express NM IIB. The endogenous expression of NM IIB in mESCs however is not sufficient to maintain cell-cell junctions in these cells when NM IIA is not expressed (Conti et al., 2004). NM IIA ablated mESCs form less compact colonies and individual cells migrate away from the colonies which show a marked reduction of E-cadherin at the cell-cell junctions. Together with findings from NM IIA knockout mice and NM IIB and IIC genetic swapping experiments the function of NM IIA in maintaining cell-cell adhesions is dependent on the level of NM IIA expression but not on its specific kinetic properties.

NM IIA in mouse placenta formation

In contrast to the visceral endoderm, the normal development of the mouse placenta requires NM IIA exclusively and neither NM IIB nor IIC can substitute for NM IIA. Ablation of either NM IIB or IIC, or even IIB and IIC together shows no obvious effects on placenta formation in mice (Ma et al., 2010). Mice ablated for NM IIA die before placenta development whereas mice expressing NM IIB (or NM IIC1) in place of NM IIA under control of the endogenous NM IIA promoter survive up to E11.5, but show major defects in

placental development manifested by a compact and underdeveloped labyrinthine layer lacking fetal blood vessel invasion (Wang et al., 2010). Moreover, homozygous mice expressing mutant p.R702C NM IIA also show similar defects in placental formation, although they are less severe than those shown by mice expressing NM IIB (or IIC1) in place of NM IIA (Zhang et al., 2012). In vitro analyses show that mutant p.R702C heavy meromyosin (HMM) IIA displays a reduction in MgATPase activity and a reduction in in vitro motility of actin-filaments compared to wild-type HMM IIA (Hu et al., 2002). Therefore, normal placenta formation requires both the proper levels of NM IIA expression as well as the full NM IIA enzymatic activity. Interactions of allantoic mesoderm with chorionic-derived trophoblasts play important roles in labyrinth morphogenesis and vascularization (Cross et al., 2006). One function of NM IIA in placental development can be attributed to its role in trophoblast-lineage cells (Crish et al., 2013). Mice specifically ablated for NM IIA in the mouse trophoblast-lineage cells demonstrate placental defects similar to mice in which NM IIA is replaced by IIB (or IIC1).

In vitro analyses of NM IIs show that the three isoforms vary significantly with respect to their enzymatic and mechanical properties. Among the three NM II isoforms, NM IIA demonstrates the highest actin-activated MgATPase activity as well as the rate of sliding actin filaments (in vitro motility) (Kim et al., 2005). Moreover, each NM II isoform exhibits a specific cellular localization encrypted in the C-terminal tail domain of the NM II isoforms (Sandquist and Means, 2008, Wang et al., 2010). Each of these unique attributes of NM IIA contributes to its specific roles for placental formation.

Regulation of NM IIA by light chain phosphorylation

NM IIA, similar to the other two isoforms present in humans, can assume two markedly different three-dimensional structures: a folded, assembly incompetent, inactive form that sediments as a faster peak in the ultracentrifuge (10S) than the asymmetric, unfolded active form (6S), which can assemble into filaments of 14–16 molecules (Figure 2). In the folded, 10S structural form three of the most critical biological properties of NM II are inhibited: bipolar filament formation, the ability of myosin to hydrolyze MgATP and the ability of myosin to slide actin filaments (Burgess et al., 2007, Jung et al., 2008, Milton et al., 2011, Wendt et al., 1999). This inhibition can be removed by phosphorylation of the 20kDa light chain on serine 19 (S-19) and threonine 18 (T-18), by a number of kinases, most prominently myosin light chain kinase (MLCK) and Rho kinase (also called Rock, Rho-associated, coiled-coil-containing protein kinase) (Figure 2). Recent work shows that MLCK is active at the periphery of the cell whereas ROCK is active at the cell center (Kassianidou et al., 2017; Totsukawa et al., 2000). Phosphorylation of the 20 kDa regulatory light chain initiates bipolar filament formation (Craig et al., 1983), markedly increases the actin-activated MgATPase activity (Adelstein and Conti, 1975, Sellers et al., 1981) and permits the sliding of actin filaments by myosin (or even sub-fragments of myosin containing the amino-terminal globular head). Each of the myosin isoforms shows differences in their MgATPase activity as well as the rate at which they slide actin filaments in the in vitro motility assay. In addition, each isoform has a particular duty ratio, the amount of time that myosin is bound to actin during a contractile cycle (Heissler and Manstein, 2013). Although there are multiple kinases that can phosphorylate S-19 and T-18, there is at present only a

single known phosphatase, protein phosphatase 1 that dephosphorylates these sites in vivo. Of note is that the activity of this phosphatase can be decreased by phosphorylation of its regulatory subunit catalyzed by Rho kinase. Thus, Rho kinase phosphorylation, unlike MLCK activity, acts to increase NM II activity by both phosphorylating the NM II regulatory light chain and inactivating the phosphatase that dephosphorylates the light chain.

In addition to the above regulatory phosphorylation of S-19 and T-18, the 20 kDa light chain of NM II can be phosphorylated by protein kinase C (PKC) on serine1,2 and threonine 9 (Figure 1B). Phosphorylation of NM II on these residues renders NM II a poorer substrate for MLCK and thus deceases NM II activity (Ikebe and Reardon, 1990, Nishikawa et al., 1984). However, unlike S-19/T-18 phosphorylation, the phosphorylation of these residues appears to be modulatory with respect to an effect on NM II activity in vivo (Beach et al., 2011b), the exception possibly being platelet derived growth factor induced reorganization of NM IIA filaments in platelets (Komatsu and Ikebe, 2007).

Regulation of NM IIA by heavy chain phosphorylation

Phosphorylation of NMHC IIA plays an important role in myosin assembly-disassembly (Dulyaninova and Bresnick, 2013). Most of the sites of heavy chain phosphorylation reside in the carboxyl-terminal end of the molecule, that is the coiled-coil and the non-helical tail piece (Figure 1B) and can be phosphorylated by a number of kinases including PKC, casein kinase II (CK II) and transient receptor potential melastatin 7 (TRPM7). Figure 1B depicts the sites in NM IIA that have been identified as phosphorylation sites. The function of heavy chain phosphorylation is either to dissociate the myosin filaments by adding the negatively charged phosphate group or to prevent filament formation (Figure 2).

Heavy chain phosphorylation of each of the NM II isoforms by PKC inhibits NM II assembly in vitro. PKC phosphorylates NMHC IIA on S-1916 near the carboxyl end of the coiled-coil. Studies with cells demonstrate that phorbol esters, which activate PKC, induce phosphorylation of NM IIA on S-1916 in platelets, T-lymphocytes and RBL-2H3 mast cells (Kawamoto et al., 1989, Moussavi et al., 1993). In mast cells phosphorylation of the various sites on NM IIA correlates with mast cell exocytosis (Ludowyke et al., 2006).

Of note is the increase in NM IIA S-1916 phosphorylation in the α-helical rod and S-1943 phosphorylation in the non-helical tailpiece following TGF-β-induced epithelial to mesenchymal transition (EMT) in mouse epithelial cells (Beach et al., 2011a). This co-ordination between NMHC IIA phosphorylation and the accompanying decreased expression of NM IIC and increased expression of NM IIB most likely contributes to the increased invasive behavior of these cells following EMT. Similarly, mesenchymal stem cells migrate randomly on a soft matrix when NM IIA is phosphorylated on S-1943, but shifting the cells to a stiffer matrix results in dephosphorylation of NMHCs IIA, permitting NM IIA filament assembly and contributing to NM IIB polarization (Raab et al., 2012). Epidermal growth factor (EGF) stimulation induces transient S-1943 phosphorylation in a variety of cell types associated with a reduction in NM IIA assembly. Experiments using breast tumor cells expressing NM IIA phosphomimetic mutants demonstrate increased cell migration and EGF-stimulated lamellipod extension as compared with cells expressing wild type NM IIA (Dulyaninova et al., 2007). Conversely, replacing wild type NM IIA with a

non-phosphorylatable tailpiece (S1943A) results in NM IIA over-assembly at the lamellar margins of spreading cells and inhibits cell migration (Beach et al., 2011b).

In a study using three different cell lines (COS-7, 4T1 and MDA-MB 231), mutation of either S-1916 or S-1943 (or both residues) to alanine blocks recruitment of GFP-NM IIA filaments to the leading-edge protrusions in 2D migration which in turn blocked maturation of anterior focal adhesions. Moreover, cells depleted of NM IIA or expressing mutant forms of GFP-NM IIA displayed severe defects in invasion and in stabilization of protrusions in 3D (Rai et al., 2017).

In addition to PKC and CK II, TRPM7 can phosphorylate all three NMHCs II. NM IIA is phosphorylated on T-1800, S-1803 and S-1808 in the coiled-coil domain and this phosphorylation reduces filament assembly in vitro and decreases the incorporation of NM IIA into the actin cytoskeleton in vivo (Clark et al., 2008a, Clark et al., 2008b).

Regulation of NM IIA by protein interactions

In addition to regulation by heavy and light chain phosphorylation, NM IIA localization and filament assembly can be modulated by interaction with other proteins such as S100A4, Lethal(2) giant larvae (Lgl1) and myosin binding protein H (Figure 2). S100A4 is a member of the S100 family of small, dimeric, EF hand proteins that function as Ca^{2+} -sensors to modulate a number of biological processes (Bresnick et al., 2015). S100A4 is also known as metastatin (mts-1) and is a well characterized metastatic factor. Calcium binding to the carboxyl-terminal EF hand induces a structural rearrangement resulting in the exposure of a hydrophobic cleft that binds to the C-terminal end of the NM IIA coiled-coil and disassembles NM IIA filaments. The overall structure of the S100A4-NM IIA peptide complex has been elucidated (Kiss et al., 2012, Ramagopal et al., 2013).

S100A4 expression is associated with enhanced cell migration, and phenotypic studies have demonstrated that S100A4 enhances chemotactic migration by maintaining cell polarization and inhibiting cell turning (Grum-Schwensen et al., 2005, Li and Bresnick, 2006). In vitro binding of S100A4 to NM IIA prevents filament formation and S100A4 binding to previously formed filaments promotes filament disassembly. Interestingly, the S1943 NM IIA residue lies outside of the NM IIA binding site for S100A4, but phosphorylation of S1943 still prevents binding of S100A4. In agreement with the in vitro regulation of NM IIA assembly by S100A4, S100A4 null macrophages over-assemble NM IIA filaments which results in reduced persistence in migration during chemotaxis (Li et al., 2010).

A second protein known to interact with NM IIA is the tumor suppressor, Lgl1 which inhibits its ability to assemble into filaments in vitro (Dahan et al., 2014, Ravid, 2014). Lgl1 also regulates the cellular localization of NM IIA and the maturation of focal adhesions. Phosphorylation of Lgl1 by aPKCζ prevents its binding to NM IIA and is important for the organization of the cellular cytoskeleton. In addition to binding to NM IIA, Lgl1 forms a complex in vivo with Par6 and aPKCζ in two different parts of the cell. Of note is that aPKCζ and NM IIA compete to bind directly to Lgl1 through the same domain. Thus Lgl1 and NM IIA appear to play a role in establishing front-rear polarity in migrating cells.

A novel actin stress fiber associated protein, LIM and calponin-homology domains1 (LIMCH1), which interacts with NM IIA but not NM IIB was identified in HeLa cells and shown to regulate NM IIA activity. The amino-terminus of LIMCH1 was found to bind to the head region of NM IIA. Depletion of LIMCH1 in HeLa cells decreases the number of actin stress fibers and focal adhesions, leading to enhanced cell migration (Lin et al., 2017).

The actin binding protein, tropomyosin 4.2 (Tpm4.2), is upregulated in rapidly migrating cells and specifically recruits NM IIA to actin filaments during stress fiber formation (Hundt et al., 2016). An investigation of how the decoration of actin filaments with Tpm4.2 affects the motor properties of NM IIA showed that in the presence of resisting loads the processive properties of NM IIA are enhanced. The authors suggest that Tpm4.2 supports NM IIA function in stress fibers by synchronizing myosin heads and enhancing load-dependent processivity.

Myosin binding protein H (MYBH) has been reported to inhibit NM IIA phosphorylation on the regulatory light chain by directly interacting with Rho kinase 1 in lung adenocarcinoma cells (Hosono et al., 2012). In addition, it was shown that MYBH can also inhibit myosin assembly by directly interacting with the rod portion of the NMHC IIA thereby reducing cell motility. The authors interpret their results to suggest that both modes of inhibition act together to reduce lung metastases. In another report, it was found that MYBH attenuates neointimal hyperplasia in a rat carotid injury model by inhibiting Rho kinase 1 (Zhu et al., 2017).

Functions specific to NM IIA

In considering whether a specific NM II isoform is associated with a specific function, it is important to recall that there are major differences in the amounts of the various isoforms in different cells and tissues. Table 1 (Ma et al., 2010) lists a variety of cells and tissues with the relative percentage of each of the NM II isoforms as determined by mass spectroscopy analysis. Most tissues are a mixture of cell types so it is not surprising to find both NM IIA and IIB in many of them. The spleen, platelets and most blood cells contain only NM IIA, though macrophages contain NM IIB too. Mature cardiac myocytes contain only NM IIB though the non-myocytes in the heart contain both NM IIA and IIB. Lung tissue is exceptional in containing equivalent amounts of NM IIA and IIC (40% each) and about one-half of this amount of IIB (Ma et al., 2010). Not only do cells contain more than one isoform but there are a number of reports showing that all three NM II isoforms can co-assemble intracellularly into heterotypic filaments in a variety of settings throughout the cell. This suggests that individual NM II isoforms could be performing both isoform-specific and isoform redundant functions when co-assembled with other NM II isoforms (Beach and Hammer, 2015, Beach et al., 2014, Shutova et al., 2014). Of note is a report showing that copolymerization of NM IIA and IIB, along with their different rates of turnover results in self-sorting of the NM IIs along the front-rear axis, resulting in a polarized actin-NM II cytoskeleton (Shutova et al., 2017). Further complicating matters is the finding that myosin 18A, a NM II lacking actin-activated MgATPase activity, can co-assemble with NM II filaments thereby expanding the functional capabilities of each (Billington et al., 2015).

In addition to genetic experiments examining substitution of one isoform of NM II for another using homologous recombination in mice, experiments using chimeric NM II isoforms have been of help in defining the requirement for the motor half of NM IIA in cells. In a study of cortical cytoskeletal pulses in cells of mesenchymal, epithelial and sarcoma origin it was determined that these pulses required phosphorylation of the 20kDa regulatory light chain for pulse contractile activity (Baird et al., 2017). Interestingly the pulses were absent from Cos-7 cells suggesting that they required NM IIA since this isoform is not present in these cells. To analyze whether it was the motor domain or the helical tail domain of IIA that was required for the pulsations, chimeras of NM IIA and IIB were used (Wang et al., 2010). These chimeras consisted of the GFP-tagged amino-terminus of the NM IIA head domain fused in frame to the NM IIB tail domain (NM II AB) and a second construct in which the GFP-N-terminus of the NM IIB head domain was fused in frame to the NM IIA tail domain (NM II BA). Analysis of time-lapse movies revealed that the pulses due to the GFP-NM IIAB chimera were similar in duration and frequency to those displayed following introduction of GFP-NM IIA into the same cell type. In contrast, the GFP-NM IIBA chimeras showed significantly lower pulse frequency and duration compared to the GFP-NM IIA controls. The results demonstrate that the NM IIA motor domain specifically, together with a tail domain capable of forming filaments, is necessary for pulsatile actomyosin dynamics. Interaction of NM IIA with a variety of proteins, including other myosins remains a promising area for further exploration.

ROLE OF *MYH9* VARIANTS IN HUMAN DISEASE: *MYH9*-RELATED DISEASE

Mutations of *MYH9* in humans cause a syndromic, autosomal-dominant disorder called *MYH9*-related disease (*MYH9*-RD) (Kelley et al., 2000; Seri et al., 2000; Kunishima et al., 2001). All affected subjects have congenital thrombocytopenia, platelet macrocytosis and inclusions of NMHC IIA in the cytoplasm of neutrophil granulocytes. In some individuals, these hematological features remain the only manifestations of the disorder throughout life. However, most *MYH9*-RD patients develop one or more late-onset manifestations of the disease, namely sensorineural deafness, kidney disease, presenile cataract, and/or elevation of liver enzymes (Pecci et al., 2014a; Pecci et al., 2012a). *MYH9*-RD encompasses five syndromic pictures previously classified as distinct disorders, i.e. May-Hegglin anomaly (MIM 155100), Sebastian syndrome (MIM 605249), Fetchner syndrome (MIM 153640), Epstein syndrome (MIM 153640), and autosomal dominant deafness DFNA17 (MIM 603622). After the identification of *MYH9* as the gene responsible for all of these nosographic entities, it was recognized that they actually represent different clinical presentations of the same disease, now known as *MYH9*-RD or *MYH9* disorder (Seri et al., 2003; Verver et al., 2015). Although *MYH9*-RD is the most frequent form of inherited thrombocytopenia, it is a rare disease. Based on data from an Italian registry, its prevalence is estimated around 3:1,000,000 (Savoia and Pecci, 2015). However, the actual prevalence is expected to be higher, as mild forms are often discovered incidentally and patients are frequently misdiagnosed with other conditions. *MYH9*-RD has been reported worldwide and there is no evidence of variation in prevalence across ethnic populations.

Clinical picture

Congenital features—The degree of thrombocytopenia varies greatly among *MYH9*-RD patients, ranging from mild reduction in platelet count to severe thrombocytopenia. Platelet count usually remains stable throughout life. Platelet function is normal and severity of bleeding tendency correlates with platelet count (Pecci et al., 2014a). Most patients have no spontaneous bleeding or only mild cutaneous bleeding (easy bruising) and are at risk for clinically significant hemorrhages only after hemostatic challenges, such as surgery or deliveries. Around 28% of patients present spontaneous mucosal bleeding, mainly menorrhagia, epistaxis, and gum bleeding (Pecci et al., 2014a). Life-threatening hemorrhages are rare.

An extreme degree of platelet macrocytosis is a hallmark of *MYH9*-RD and represents a crucial clue to the identification of these patients (Figure 4A, B). In fact, platelet macrocytosis is much more marked than in acquired thrombocytopenias and most of the other forms of inherited thrombocytopenia (Noris et al., 2014). Giant platelets (platelets larger than erythrocytes) are always present at the examination of blood smears. Routine automated cell counters do not recognize the very large platelets of *MYH9*-RD patients and thus overestimate the degree of thrombocytopenia and often do not detect the platelet macrocytosis (Noris et al., 2013). Microscopic or flow cytometry counting of platelets is therefore required for correct measurement of platelet count of *MYH9*-RD individuals and microscopic examination of blood smears is essential for the identification of the prominent platelet macrocytosis (Seri et al., 2003).

Inclusions of the NMHC IIA protein may be identified after conventional staining of blood smears in 42–84% of *MYH9*-RD patients (Seri et al., 2003). They appear as faint, mildly basophilic inclusions, called Döhle-like bodies, which can be observed in the cytoplasm of 15–100% of neutrophil granulocytes (Figure 4C). However, the inclusions can be clearly detected in all neutrophils of all *MYH9*-RD patients after immunofluorescence staining for the MYH9 protein (Figure 4, D–F). For this reason, immunofluorescence assay for NMHC IIA on peripheral blood smear has been proposed and validated as a diagnostic test for *MYH9*-RD and today represents the gold standard for the identification of these patients. Several groups showed that this assay has a close to 100% specificity and sensitivity for the diagnosis (Kunishima et al., 2003; Savoia et al., 2010; Kitamura et al., 2009; Greinacher et al., 2017).

Late-onset manifestations—Hearing loss is the most frequent late-onset feature. The analysis of a large series of *MYH9*-RD patients showed that it is present in about 50% of cases at a mean age of 33 years and is expected to occur in almost all patients over time (Pecci et al., 2014a). The age at onset is homogenously distributed along the first to sixth decades. Features are those of a bilateral sensorineural hearing loss that is often progressive (Verver et al., 2016). At onset or in mild forms, hearing impairment affects mainly the high and mid tones, but in advanced or more severe forms it involves all frequencies. Forms with onset in childhood or adolescence usually show severe evolution and lead to severe or profound deafness. Kidney damage occurs in about 25% of *MYH9*-RD patients as a progressive proteinuric nephropathy. In most cases, nephropathy occurs before the age of 35

(mean age at onset, 27 years) and presents an aggressive course, as it evolves within a few years into end-stage renal disease requiring dialysis or kidney transplantation (Pecci et al., 2014a). In some cases, proteinuria may appear later in life and/or show a slower progression (Rocca et al., 1993; Han et al., 2011).

Presenile cataracts affects about 20% of patients. Mean age at onset is 37 years; congenital forms have also been reported (Peterson et al., 1985; De Rocco et al., 2009). In most cases (75%) cataracts are bilateral (Pecci et al., 2014a).

About half of *MYH9*-RD patients present chronic or intermittent elevation of liver enzymes, especially transaminases and gamma-glutamyl transferase. This alteration seems benign since no patients have been reported to show evolution to liver dysfunction to date (Pecci et al., 2012a).

Diagnosis—*MYH9*-RD is easily suspected whenever the dominant inheritance of thrombocytopenia and the marked platelet macrocytosis are disclosed. Diagnostic suspicion is even stronger when thrombocytopenia associates with the extra-hematological features of the disease. However, *MYH9*-RD patients are frequently misdiagnosed with immune thrombocytopenia (ITP), the most frequent form of acquired thrombocytopenia, indicating that distinguishing between these patients is difficult. Misdiagnosis with ITP often leads to administration of undue immunosuppressive therapies. Among patients enrolled in the Italian registry, about 60% of index cases received a previous diagnosis of ITP, 30% inappropriate treatments, and 12% an unnecessary splenectomy (unpublished observations). Diagnostic difficulties derive from the high frequency of sporadic cases and the fact that the low platelet count is often discovered only in adulthood, two factors that can make it difficult to recognize the genetic origin of thrombocytopenia. The failure of routine automated counters in detecting platelet macrocytosis also contributes to mistaken diagnoses. Once *MYH9*-RD is suspected, diagnosis can be confirmed by immunofluorescence assay for NMHC IIA on peripheral blood smear. The identification of the causative *MYH9* mutation is not strictly required in the presence of typical NMHC IIA leukocyte inclusions, however, it is important for providing prognostic assessment (see below, genotype-phenotype correlations).

Mutation spectrum

More than 80 different mutations have been identified in families affected with *MYH9*-RD (reviewed in Table 2). In most cases, they are single nucleotide substitutions that affect either the head domain or the coiled-coil region of the tail domain. In the head domain, the most frequently affected residue is arginine 702 located in the short functional SH1 helix. Many head domain mutations other than the R702 substitutions appear to cluster in a distinct hydrophobic seam at the interface between the SH3 motif and the upper 50 kDa subdomain (Kahr et al., 2009; Pecci et al., 2014a). In about 20% of families, the disease is caused by splicing, nonsense or frameshift mutations that affect intron 40 or exon 41, and results in alterations of a variable portion of the non-helical tailpiece (Pecci et al., 2014a; Saposnik et al., 2014; Kunishima et al., 2003). In a few cases, the causative mutation is an in-frame deletion or duplication, frequently in exon 25, where they are likely to occur because of the

presence of repetitive sequences. Of note is that almost 70% of families have mutations affecting only 6 residues: serine 96 and arginine 702 of the head domain, arginine 1165, aspartate 1424, and glutamine 1841 of the coiled-coil, or arginine 1933 of the non-helical tailpiece.

Although *MYH9*-RD is transmitted as an autosomal-dominant trait, about 35% of index cases are sporadic (Savoia et al., 2010). In more than half of these cases, a *de novo* mutation was confirmed by segregation analysis in the parents. Characterization of somatic or germinal mosaicism explains a few sporadic cases, which might be more frequent if it were possible to analyse more biological samples from apparently healthy family members (Kunishima et al., 2005; Kunishima et al., 2009; Kunishima et al., 2014; Gresele et al., 2013).

Genotype-phenotype correlations

The risk of developing late-onset manifestations of *MYH9*-RD and their severity are dependent on the specific *MYH9* mutation (Dong et al., 2005; Pecci et al., 2008a; Pecci et al., 2014a; Verver et al., 2016). A recent analysis of 255 consecutive patients identified statistically significant genotype-phenotype correlations and defined the disease evolution associated with 7 *MYH9* genotypes, which, together, are responsible for about 85% of disease cases (Pecci et al., 2014a). The amino acid substitutions of arginine at residue 702 of the head domain are associated with the most severe evolution: all patients carrying these mutations develop end-stage renal disease and severe deafness before the fourth decade (Pecci et al., 2014a; Verver et al., 2016; Sekine et al., 2010). The p.D1424H mutation in the coiled-coil region results in a relatively high risk of developing the late-onset manifestations. The mutations affecting the interface between the SH3 motif and the upper 50 kDa subdomain of the head domain are associated with high risk of deafness but low risk of kidney damage or cataract. A similar phenotype derives from the substitutions of the arginine 1165 of the coiled-coil. Finally, the p.D1424N and p.E1841K *missense* substitutions, as well as the frameshift or nonsense alterations affecting the non-helical tailpiece are associated with a low risk of the extra-hematological features. Thus, in patients carrying these mutations, thrombocytopenia usually remains the only feature of the disease throughout life or associates only with mild and late-onset hearing defect (Pecci et al., 2014a; Verver et al., 2016). Regarding platelet phenotype, patients with mutations affecting the head domain have more severe thrombocytopenia and larger platelets than those carrying alterations in the tail domain (Pecci et al., 2014a; Noris et al., 2014; Kunishima et al., 2007). Mean platelet count is approximately 30 $\times 10^9$/L in patients with head domain mutations and 80 $\times 10^9$/L in those with tail domain variants; as a consequence, individuals with head domain mutations have a more severe bleeding tendency (Pecci et al., 2014a). Finally, genotype-phenotype correlations have also been reported for the morphological features of leukocyte NM IIA aggregates following immunofluorescence staining (Kunishima et al., 2003; Miyazaki et al., 2009; Savoia et al., 2010).

Pathogenesis

Macrothrombocytopenia in *MYH9*-RD derives from defects of the late events of platelet biogenesis, i.e. the formation of proplatelets from mature megakaryocytes and the release of

platelets from proplatelet free ends (or tips) (Kaushansky, 2015). NM IIA is dispensable for megakaryocyte differentiation and maturation (Chen et al., 2007) and patients with *MYH9*-RD show normal production of fully-developed megakaryocytes (Heynen et al., 1998; Pecci et al., 2009). However, megakaryocytes of *MYH9*-RD individuals present a profound alteration of the morphology of proplatelets, including an evident defect in branching and increased diameter of the buds at the proplatelets tips (Pecci et al., 2009). Consistently, mouse models that closely reproduce the phenotype of the human disease show normal or increased production of mature megakaryocytes and alteration of proplatelets formation *in vitro* and *in vivo* (Zhang et al., 2012; Suzuki et al., 2013). The morphology of proplatelets of these mice appears very similar to that observed in *MYH9*-RD patients. The defect of proplatelets branching contributes to thrombocytopenia, as it results in a reduced number of free ends that generates platelets (Italiano et al., 1999; Thon and Italiano, 2012). The increased size of proplatelet tips correlates with platelet macrocytosis (Pecci et al., 2009; Zhang et al., 2012) and reflects the impairment of the constrictive force generated by the actomyosin cytoskeleton that splits platelets from proplatelets free ends and limits platelet size (Thon et al., 2012; Thon and Italiano, 2012a; Badirou et al., 2015).

Even an ectopic platelet release within the bone marrow could contribute to defective platelet biogenesis of *MYH9*-RD. In fact, NM IIA mediates the suppression of proplatelets extension exerted by megakaryocyte adhesion to type I collagen through integrin α2β1 (Chen et al., 2007; Balduini et al., 2008). This mechanism serves to prevent megakaryocytes from extending proplatelets before they reach the sinusoids during their migration within the bone marrow (Chen et al., 2007; Larson and Watson, 2006), and is defective in *MYH9*-RD patients (Pecci et al., 2009). Mutations responsible for *MYH9*-RD also reduce the ability of megakaryocytes to migrate on type I collagen, an effect that may contribute to ectopic platelet release (Pecci et al., 2011).

Investigations of the pathogenesis of nephropathy suggested that *MYH9* mutations cause proteinuria and progressive glomerulosclerosis deriving from defects in the function of the podocytes, highly specialized kidney epithelial cells that have a central role in glomerular filtration. Mouse knock-in mutant models reproducing the human disease present focal segmental glomerulosclerosis associated with signs of podocyte injury, such as effacement of the podocyte foot processes and loss of the filtration slits between the foot processes (Zhang et al., 2012; Chechova et al., 2018). Interestingly, a similar phenotype was induced in mice through the ablation of NMHC IIA exclusively in the podocytes (Zhang et al., 2012). Primary podocytes isolated from a mouse knock-in mutant model showed altered structure and reorganization of the actomyosin cytoskeleton along with increased motility *in vitro*, a functional alteration that reflects podocyte foot effacement *in vivo* (Chechova et al., 2018). The abnormalities observed in mutant mice closely resemble those found in kidney biopsies of *MYH9*-RD patients (Sekine et al., 2010; Kopp, 2010). The mechanisms of hearing loss caused by *MYH9* mutations are poorly understood. Studies of the mouse cochlea showed that NM IIA is localized in the hair cells of the organ of Corti, the spiral ligament and the spiral limbus. In the hair cells, NM IIA is strongly expressed within the stereocilia, the structures whose movement triggers transduction of the sound stimulus into electric signals directed to the brain (Mhatre et al., 2006; Lalwani et al., 2008). Mouse models of human deafness caused by mutations in three other myosins (myosins VI, VIIa

and XVA) indicated that structural abnormalities of the stereocilia were the common feature underlying hearing loss. This led to the hypothesis that *MYH9* mutations also cause deafness by disrupting the structural integrity of stereocilia (Mhatre et al., 2006; Ebrahim et al., 2013). Pathogenesis of cataract and liver enzymes alteration is completely unknown.

Therapy

For many years, treatment of thrombocytopenia in *MYH9*-RD patients has been similar to that of most other forms of inherited thrombocytopenia, essentially based on general measures to prevent bleeding, empirical administration of drugs improving hemostasis (antifibrinolytics or desmopressin), and platelet transfusions (Balduini et al., 2013). In recent years, eltrombopag, a drug that stimulates platelet production by activating the thrombopoietin receptor and is licensed for treatment of some forms of acquired thrombocytopenia, has been successfully tested in *MYH9*-RD patients. A phase 2 clinical trial showed that short-term eltrombopag was highly effective in increasing the platelet count in 11 out of 12 individuals with *MYH9*-RD and severe thrombocytopenia. The drug induced remission of spontaneous hemorrhages in all the patients with bleeding symptoms at baseline (Pecci et al., 2010). Based on these results, eltrombopag was successfully used for preparing patients with severe *MYH9*-related thrombocytopenia for elective surgery (Pecci et al., 2012b; Favier et al., 2013; Favier et al., 2017). Romiplostim, another agonist of the thrombopoietin receptor was also used for this purpose in one *MYH9*-RD patient (Yamanouchi et al., 2015). Dialysis and kidney transplantation are the only possible treatments for *MYH9*-RD patients with end-stage renal disease. Some observations suggested that drugs that block the renin-angiotensin system reduce proteinuria in *MYH9*-RD individuals presenting with early-stage kidney involvement (Pecci et al., 2008b; Sekine et al., 2010). Long-term benefit of this treatment on the progression of kidney damage is still to be assessed.

Cochlear implantation is highly effective in restoring hearing function in *MYH9*-RD patients who develop severe to profound deafness (Pecci et al., 2014b).

MYH9 VARIANTS IN OTHER HUMAN DISEASES

A role for *MYH9* has been suggested in human diseases other than *MYH9*-RD. In particular, inherited variants in *MYH9* have been associated with predisposition to chronic kidney disease and non-syndromic hearing loss. Recent studies in mice provide evidence that *Myh9* acts as a tumor suppressor in certain types of cancer, suggesting that defects of *MYH9* could contribute to oncogenesis in the corresponding human diseases.

Chronic kidney disease

Chronic kidney disease is more prevalent in populations of African ancestry than in those of European or Asian origin. In 2008, genetic variations in *MYH9* were found to be associated with non-diabetic end-stage renal disease and focal segmental glomerulosclerosis in African Americans. In particular, a set of SNPs close to the 3′ end of *MYH9*, reported as haplotype E1, was associated with the strongest risk according to a recessive inheritance model. This haplotype was much more frequent in African than in European Americans and the

association fully explained the increased burden of kidney disease among individuals of African origin (Kopp et al., 2008; Kao et al., 2008). However, no mutations in *MYH9* with potentially causal effects have been characterized so far. In 2010, the association of the 22q12.3 region with non-diabetic kidney disease in African Americans was re-evaluated using the dataset of the 1000 Genome Project. The study concluded that the association was actually due to two distinct sets of variants in the apolipoprotein L1 (*APOL1*) gene, the haplotypes G1 and G2, which are located approximately 20 kb downstream of the 3′ end of *MYH9*. All the previously reported associations with *MYH9* variations were explained by strong linkage disequilibrium with these two *APOL1* haplotypes (Genovese et al., 2010). Further studies confirmed these findings (Tzur et al., 2010; Kopp et al., 2011). Moreover, a recent investigation showed that transgenic podocyte-specific expression of APOL1 G1 and G2 in mice induces kidney damage that closely resemble the human disease (Beckerman et al., 2017). Nevertheless, a few studies suggested further associations of *MYH9* with specific forms of chronic kidney disease that appear to be independent of the linkage with *APOL1* G1 and G2. In particular, associations were identified between some SNPs in *MYH9* and nephropathy in the European and Asian populations, in which APOL1 G1 and G2 are almost absent (Cooke et al., 2012; Cheng et al., 2011; O'Seaghdha et al., 2011). Whether additional high-risk variants are localized in *MYH9* or these SNPs are tagging variants in the neighboring *APOL1* to *APOL6* gene region is still unknown and justifies further investigation.

Sensorineural deafness

Inherited *MYH9* variants have been identified in a few families with non-syndromic hearing loss (Table 3). In most of these cases, deafness was transmitted as a dominant trait and had the features of a bilateral and progressive sensorineural defect that predominantly involves the mid and high frequencies, similar to the hearing loss of *MYH9*-RD patients. We cannot exclude the possibility that some of these variants actually cause *MYH9*-RD presenting with deafness as the most prominent feature. In fact, the p.R705H mutation of MYH9 was initially associated with the non-syndromic deafness DFNA17 (Lalwani et al., 2000), whereas subsequent studies showed that this variant actually induces a form of *MYH9*-RD characterized by mild thrombocytopenia, severe deafness and a very low risk of the other disease manifestations (Verver et al., 2015). However, in some of the patients reported in Table 3, hematological, kidney or lens abnormalities were excluded (Wu et al., 2013; Sloan-Heggen et al., 2016), indicating that *MYH9* could be involved in non-syndromic deafness.

Cancer

Several investigations suggested that *MYH9* plays a role in cancer. Many of these studies propose that NM IIA expression or its functions in neoplastic cells promote the progression of various types of cancers (Derycke et al., 2011; Katono et al., 2015; Liao et al., 2017; Ye et al., 2017). However, the investigations that obtained the strongest evidence of a driving role of *MYH9* alterations in oncogenesis found that this gene acts as a tumor suppressor. Schramek et al. searched for squamous cell carcinoma (SCC) driver mutations through an *in vivo* RNA interference screen in which epithelial cell-specific delivery of silencing RNA was carried out *in utero* on pregnant mice. In animals predisposed to SCC because of TGFβ-receptor-II conditional knockout, silencing *Myh9* induced metastatic SCCs in the skin and

head and neck with median latencies of 3 to 7 months. Ablation of *Myh9* also led to development of skin SCC in 30% of TGFβ-receptor-II wild-type mice after 1-year observation. Investigation of mouse and human keratinocytes showed that NM IIA deficiency, or inhibition of its ATPase activity, induce defective activation of the p53 protein upon DNA damage, as a result of impaired p53 stability and nuclear localization. The authors found that 24–31% of human skin and head and neck SCCs are characterized by no or very weak NM IIA expression. Analysis of data from The Cancer Genome Atlas indicated that low *MYH9* RNA expression associates with poor survival in patients with head and neck SCC, thus also supporting a role for *MYH9* as a tumor suppressor in humans. *MYH9* is mutated in 5% of human head and neck SCCs, and hemizygous *MYH9* loss is present in 15% of these tumors. Most of the *MYH9* mutations cluster in the ATPase domain and were found to impair an *in vitro* p53 response to DNA damage (Schramek et al., 2014). Interestingly, another mouse model, in which *Myh9* was ablated in the heart and the tongue epithelium, showed the development of tongue SCC (Conti et al., 2015). SCC occurred very early during embryonic epithelium development, with a 100% penetrance, and on a wild-type background. In this model, oncogenesis was independent of defective p53 activation. Recently, Kas and colleagues searched for mutations driving the development of invasive lobular breast carcinoma (ILC) through an insertional mutagenesis screen in E-cadherin conditional knockout mice. The authors found that mutations resulting in heterozygous loss of *Myh9* act as driver events for the development of tumors recapitulating the features of human ILC (Kas et al., 2017). Consistently, inactivation of *Myh9* in mammary glands by *in situ* gene editing induced the rapid development of ILC in these mice. The effects of *Myh9* haploinsufficiency were not mediated by an altered p53 response in this mouse model either, suggesting that alternative mechanisms are involved in oncogenesis driven by *Myh9* deficiency. The Cancer Genome Atlas showed that *MYH9* is aberrant in 46% of human ILCs and that most mutations correlate with reduced mRNA expression.

FINAL REMARKS

MYH9 encodes the heavy chain of NM IIA, a cytoplasmic myosin that plays a major role in human development and disease. Mutations of *MYH9* cause an autosomal-dominant disorder, *MYH9*-RD, characterized by thrombocytopenia with giant platelets and a variable risk of developing kidney damage, sensorineural deafness, cataracts, and/or abnormalities of liver enzymes. Moreover, NM IIA appears to act as a tumor suppressor and loss of the *MYH9* gene has been associated with epithelial cancers in both mice and humans. Although many functional roles of NM IIA have been elucidated, our knowledge of the pathogenetic mechanisms responsible for the different diseases is limited. Since current evidence suggests that the genetic manipulation at the *MYH9* locus recapitulates the human phenotypes in mice, these animals are good models for studying the role of NM IIA in different organs and how mutations lead to pathological phenotypes, including *MYH9*-driven oncogenesis. Future work in this field should result in important new insights into a number of different disease mechanisms related to abnormalities in the *MYH9* gene and its gene product, NM IIA.

Acknowledgments

This review and the corresponding Gene Wiki article are written as part of the Gene Wiki Review series--a series resulting from a collaboration between the journal GENE and the Gene Wiki Initiative. The Gene Wiki Initiative is supported by National Institutes of Health (GM089820). Additional support for Gene Wiki Reviews is provided by Elsevier, the publisher of GENE. The authors would like to thank Dr. Sachiyo Kawamoto and Dr. Mary Anne Conti who kindly read the manuscript.

The corresponding Gene Wiki entry for this review can be found here: https://en.wikipedia.org/wiki/MYH9

FUNDING SOURCES

The work of Alessandro Pecci is supported by the Telethon Foundation (grant n. GGP17106) and by the IRCCS Policlinico San Matteo Foundation. The work of Xuefei Ma and Robert S. Adelstein is supported by the NHLBI Division of Intramural Research, NIH, Bethesda MD. The work of Anna Savoia is supported by IRCCS Burlo Garofolo.

References

Adelstein RS, Conti MA. Phosphorylation of platelet myosin increases actin-activated myosin ATPase activity. Nature. 1975; 256:597–598. [PubMed: 170529]

Badirou I, Pan J, Souquere S, Legrand C, Pierron G, Wang A, Eckly A, Roy A, Gachet C, Vainchenker W, Chang Y, Léon C. Distinct localizations and roles of non-muscle myosin II during proplatelet formation and platelet release. J Thromb Haemost. 2015; 13:851–859. [PubMed: 25736522]

Baird MA, Billington N, Wang A, Adelstein RS, Sellers JR, Fischer RS, Waterman CM. Local pulsatile contractions are an intrinsic property of the myosin 2A motor in the cortical cytoskeleton of adherent cells. Mol Biol Cell. 2017; 28:240–251. [PubMed: 27881665]

Balduini A, Pallotta I, Malara A, Lova P, Pecci A, Viarengo G, Balduini CL, Torti M. Adhesive receptors, extracellular proteins and myosin IIA orchestrate proplatelet formation by human megakaryocytes. J Thromb Haemost. 2008; 6:1900–1907. [PubMed: 18752571]

Balduini CL, Pecci A, Noris P. Diagnosis and management of inherited thrombocytopenias. Semin Thromb Hemost. 2013; 39:161–171. [PubMed: 23397552]

Beach JR, Hussey GS, Miller TE, Chaudhury A, Patel P, Monslow J, Zheng Q, Keri RA, Reizes O, Bresnick AR, Howe PH, Egelhoff TT. Myosin II isoform switching mediates invasiveness after TGF-beta-induced epithelial-mesenchymal transition. Proc Natl Acad Sci U S A. 2011a; 108:17991–17996. [PubMed: 22025714]

Beach JR, Licate LS, Crish JF, Egelhoff TT. Analysis of the role of Ser1/Ser2/Thr9 phosphorylation on myosin II assembly and function in live cells. BMC Cell Biol. 2011b; 12:52. [PubMed: 22136066]

Beach JR, Shao L, Remmert K, Li D, Betzig E, Hammer JA 3RD. Nonmuscle myosin II isoforms coassemble in living cells. Curr Biol. 2014; 24:1160–1166. [PubMed: 24814144]

Beach JR, Hammer JA 3RD. Myosin II isoform co-assembly and differential regulation in mammalian systems. Exp Cell Res. 2015; 334:2–9. [PubMed: 25655283]

Beckerman P, Bi-karchin J, Park AS, Qiu C, Dummer PD, Soomro I, Boustany-Kari CM, Pullen SS, Miner JH, Hu CA, Rohacs T, Inoue K, Ishibe S, Saleem MA, Palmer MB, Cuervo AM, Kopp JB, Susztak K. Transgenic expression of human APOL1 risk variants in podocytes induces kidney disease in mice. Nat Med. 2017; 23:429–438. [PubMed: 28218918]

Billington N, Beach JR, Heissler SM, Remmert K, Guzik-Lendrum S, Nagy A, Takagi Y, Shao L, Li D, Yang Y, Zhang Y, Barzik M, Betzig E, Hammer JA 3RD, Sellers JR. Myosin 18A coassembles with nonmuscle myosin 2 to form mixed bipolar filaments. Curr Biol. 2015; 25:942–948. [PubMed: 25754640]

Bresnick AR, Weber DJ, Zimmer DB. S100 proteins in cancer. Nat rev cancer. 2015; 15:96–109. [PubMed: 25614008]

Burgess SA, Yu S, Walker ML, Hawkins RJ, Chalovich JM, Knight PJ. Structures of smooth muscle myosin and heavy meromyosin in the folded, shutdown state. J Mol Biol. 2007; 372:1165–1178. [PubMed: 17707861]

Cechova S, Dong F, Chan F, Kelley MJ, Ruiz P, Le TH. MYH9 E1841K Mutation Augments Proteinuria and Podocyte Injury and Migration. J Am Soc Nephrol. 2018; 29:155–167. [PubMed: 28993503]

Chen Z, Naveiras O, Balduini A, Mammoto A, Conti MA, Adelstein RS, Ingber D, Daley GQ, Shivdasani RA. The May-Hegglin anomaly gene MYH9 is a negative regulator of platelet biogenesis modulated by the Rho-ROCK pathway. Blood. 2007; 110:171–179. [PubMed: 17392504]

Cheng W, Zhou X, Zhu L, Shi S, Lv J, Liu L, Zhang H. Polymorphisms in the nonmuscle myosin heavy chain 9 gene (MYH9) are associated with the progression of IgA nephropathy in Chinese. Nephrol Dial Transplant. 2011; 26:2544–2549. [PubMed: 21245129]

Clark K, Middelbeek J, Dorovkov MV, Figdor CG, Ryazanov AG, Lasonder E, Van Leeuwen FN. The alpha-kinases TRPM6 and TRPM7, but not eEF-2 kinase, phosphorylate the assembly domain of myosin IIA, IIB and IIC. FEBS Lett. 2008a; 582:2993–2997. [PubMed: 18675813]

Clark K, Middelbeek J, Lasonder E, Dulyaninova NG, Morrice NA, Ryazanov AG, Bresnick AR, Figdor CG, Van Leeuwen FN. TRPM7 regulates myosin IIA filament stability and protein localization by heavy chain phosphorylation. J Mol Biol. 2008b; 378:790–803. [PubMed: 18394644]

Conti MA, Even-Ram S, Liu C, Yamada KM, Adelstein RS. Defects in cell adhesion and the visceral endoderm following ablation of nonmuscle myosin heavy chain II-A in mice. J Biol Chem. 2004; 279:41263–41266. [PubMed: 15292239]

Conti MA, Saleh AD, Brinster LR, Cheng H, Chen Z, Cornelius S, Liu C, Ma X, Van Waes C, Adelstein RS. Conditional deletion of nonmuscle myosin II-A in mouse tongue epithelium results in squamous cell carcinoma. Sci Rep. 2015; 5:14068. [PubMed: 26369831]

Cooke JN, Bostrom MA, Hicks PJ, Ng MC, Hellwege JN, Comeau ME, Divers J, Langefeld CD, Freedman BI, Bowden DW. Polymorphisms in MYH9 are associated with diabetic nephropathy in European Americans. Nephrol Dial Transplant. 2012; 27:1505–1511. [PubMed: 21968013]

Craig R, Smith R, Kendrick-Jones J. Light-chain phosphorylation controls the conformation of vertebrate non-muscle and smooth muscle myosin molecules. Nature. 1983; 302:436–439. [PubMed: 6687627]

Crish J, Conti MA, Sakai T, Adelstein RS, Egelhoff TT. Keratin 5-Cre-driven excision of nonmuscle myosin IIA in early embryo trophectoderm leads to placenta defects and embryonic lethality. Dev Biol. 2013; 382:136–248. [PubMed: 23911870]

Cross JC, Nakano H, Natale DR, Simmons DG, Watson ED. Branching morphogenesis during development of placental villi. Differentiation. 2006; 74:393–401. [PubMed: 16916377]

D'Apolito M, Guarnieri V, Boncristiano M, Zelante L, Savoia A. Cloning of the murine nonmuscle heavy chain myosin IIA gene, ortholog of human MYH9 responsible for May-Hegglin, Sebastian, Fechtner, and Epstein syndromes. Gene. 2002; 286:215–222. [PubMed: 11943476]

Dahan I, Petrov D, Cohen-Kfir E, Ravid S. The tumor suppressor Lgl1 forms discrete complexes with NMII-A and Par6alpha-aPKCzeta that are affected by Lgl1 phosphorylation. J Cell Sci. 2014; 127:295–304. [PubMed: 24213535]

De Rocco D, Pujol-Moix N, Pecci A, Faletra F, Bozzi V, Balduini CL, Savoia A. Identification of the first duplication in MYH9-related disease: a hot spot for unequal crossing-over within exon 24 of the MYH9 gene. Eur J Med Genet. 2009; 52:191–194. [PubMed: 19450438]

Derycke L, Stove C, Vercoutter-Edouart AS, De Wever O, Dollé L, Colpaert N, Depypere H, Michalski JC, Bracke M. The role of non-muscle myosin IIA in aggregation and invasion of human MCF-7 breast cancer cells. Int J Dev Biol. 2011; 55:835–840. [PubMed: 22161839]

Dong F, Li S, Pujol-Moix N, Luban NL, Shin SW, Seo JH, Ruiz-Saez A, Demeter J, Langdon S, Kelley MJ. Genotype-phenotype correlation in MYH9-relatedthrombocytopenia. Br J Haematol. 2005; 130:620–627. [PubMed: 16098078]

Dulyaninova NG, House RP, Betapudi V, Bresnick AR. Myosin-IIA heavy-chain phosphorylation regulates the motility of MDA-MB-231 carcinoma cells. Mol Biol Cell. 2007; 18:3144–3155. [PubMed: 17567956]

Dulyaninova NG, Bresnick AR. The heavy chain has its day: regulation of myosin-II assembly. Bioarchitecture. 2013; 3:77–85. [PubMed: 24002531]

Ebrahim S, Fujita T, Millis BA, Kozin E, Ma X, Kawamoto S, Baird MA, Davidson M, Yonemura S, Hisa Y, Conti MA, Adelstein RS, Sakaguchi H, Kachar B. NMII forms a contractile transcellular sarcomeric network to regulate apical cell junctions and tissue geometry. Curr Biol. 2013; 23:731–736. [PubMed: 23562268]

Eddinger TJ, Meer DP. Myosin II isoforms in smooth muscle: heterogeneity and function. Am J Physiol Cell Physiol. 2007; 293:C493–508. [PubMed: 17475667]

Favier R, Feriel J, Favier M, Denoyelle F, Martignetti JA. First successful use of eltrombopag before surgery in a child with MYH9-related thrombocytopenia. Pediatrics. 2013; 132:e793–795. [PubMed: 23940247]

Favier R, De Carne C, Elefant E, Lapusneanu R, Gkalea V, Rigouzzo A. Eltrombopag to Treat Thrombocytopenia During Last Month of Pregnancy in a Woman With MYH9-Related Disease: A Case Report. A A Pract. 2018; 10:10–12. [PubMed: 28795988]

Foth BJ, Goedecke MC, Soldati D. New insights into myosin evolution and classification. Proc Natl Acad Sci USA. 2006; 103:3681–3686. [PubMed: 16505385]

Genovese G, Friedman DJ, Ross MD, Lecordier L, Uzureau P, Freedman BI, Bowden DW, Langefeld CD, Oleksyk TK, Uscinski Knob AL, Bernhardy AJ, Hicks PJ, Nelson GW, Vanhollebeke B, Winkler CA, Kopp JB, Pays E, Pollak MR. Association of trypanolytic ApoL1 variants with kidney disease in African Americans. Science. 2010; 329:841–845. [PubMed: 20647424]

Golomb E, Ma X, Jana SS, Preston YA, Kawamoto S, Shoham NG, Goldin E, Conti MA, Sellers JR, Adelstein RS. Identification and characterization of nonmuscle myosin II-C, a new member of the myosin II family. J Biol Chem. 2004; 279:2800–2808. [PubMed: 14594953]

Greinacher A, Pecci A, Kunishima S, Althaus K, Nurden P, Balduini CL, Bakchoul T. Diagnosis of inherited platelet disorders on a blood smear: a tool to facilitate worldwide diagnosis of platelet disorders. J Thromb Haemost. 2017; 15:1511–1521. [PubMed: 28457011]

Gresele P, De Rocco D, Bury L, Fierro T, Mezzasoma AM, Pecci A, Savoia A. Apparent genotype-phenotype mismatch in a patient with MYH9-related disease: when the exception proves the rule. Thromb Haemost. 2013; 110:618–620. [PubMed: 23925420]

Grum-Schwensen B, Klingelhofer J, Berg CH, El-naaman C, Grigorian M, Lukanidin E, Ambartsumian N. Suppression of tumor development and metastasis formation in mice lacking the S100A4(mts1) gene. Cancer Res. 2005; 65:3772–3780. [PubMed: 15867373]

Han KH, Lee H, Kang HG, Moon KC, Lee JH, Park YS, Ha IS, Ahn HS, Choi Y, Cheong HI. Renal manifestations of patients with MYH9-related disorders. Pediatr Nephrol. 2011; 26:549–555. [PubMed: 21210153]

Heissler SM, Manstein DJ. Nonmuscle myosin-2: mix and match. Cell Mol Life Sci. 2013; 70:1–21. [PubMed: 22565821]

Heissler SM, Sellers JR. Kinetic Adaptations of Myosins for Their Diverse Cellular Functions. Traffic. 2016; 17:839–859. [PubMed: 26929436]

Hosono Y, Usukura J, Yamaguchi T, Yanagisawa K, Suzuki M, Takahashi T. MYBPH inhibits NM IIA assembly via direct interaction with NMHC IIA and reduces cell motility. Biochem Biophys Res Commun. 2012; 428:173–178. [PubMed: 23068101]

Hu A, Wang F, Sellers JR. Mutations in human nonmuscle myosin IIA found in patients with May-Hegglin anomaly and Fechtner syndrome result in impaired enzymatic function. J Biol Chem. 2002; 277:46512–46517. [PubMed: 12237319]

Hundt N, Steffen W, Pathan-Chhatbar S, Taft MH, Manstein DJ. Load-dependent modulation of non-muscle myosin-2A function by tropomyosin 4.2. Sci Rep. 2016; 6:20554. [PubMed: 26847712]

Ikebe M, Reardon S. Phosphorylation of bovine platelet myosin by protein kinase C. Biochemistry. 1990; 29:2713–2720. [PubMed: 2346743]

Italiano JE Jr, Lecine P, Shivdasani RA, Hartwig JH. Blood platelets are assembled principally at the ends of proplatelet processes produced by differentiated megakaryocytes. Journal of Cell Biology. 1999; 147:1299–1312. [PubMed: 10601342]

Jung HS, Komatsu S, Ikebe M, Craig R. Head-head and head-tail interaction: a general mechanism for switching off myosin II activity in cells. Mol Biol Cell. 2008; 19:3234–3242. [PubMed: 18495867]

Kahr WH, Savoia A, Pluthero FG, Li L, Christensen H, De Rocco D, Traivaree C, Butchart SE, Curtin J, Stollar EJ, Forman-Kay JD, Blanchette VS. Megakaryocyte and platelet abnormalities in a patient with a W33C mutation in the conserved SH3-like domain of myosin heavy chain IIA. Thromb Haemost. 2009; 102:1241–1250. [PubMed: 19967157]

Kao WH, Klag MJ, Meoni LA, Reich D, Berthier-Schaad Y, Li M, Coresh J, Patterson N, Tandon A, Powe NR, Fink NE, Sadler JH, Weir MR, Abboud HE, Adler SG, Divers J, Iyengar SK, Freedman BI, Kimmel PL, Knowler WC, Kohn OF, Kramp K, Leehey DJ, Nicholas SB, Pahl MV, Schelling JR, Sedor JR, Thornley-Brown D, Winkler CA, Smith MW, Parekh RS. Family Investigation of Nephropathy and Diabetes Research Group. MYH9 is associated with nondiabetic end-stage renal disease in African Americans. Nat Genet. 2008; 40:1185–1192. [PubMed: 18794854]

Kas SM, de Ruiter JR, Schipper K, Annunziato S, Schut E, Klarenbeek S, Drenth AP, van der Burg E, Klijn C, Ten Hoeve JJ, Adams DJ, Koudijs MJ, Wesseling J, Nethe M, Wessels LFA, Jonkers J. Insertional mutagenesis identifies drivers of a novel oncogenic pathway in invasive lobular breast carcinoma. Nat Genet. 2017; 49:1219–1230. [PubMed: 28650484]

Kassianidou E, Hughes JH, Kumar S. Activation of ROCK and MLCK tunes regional stress fiber formation and mechanics via preferential myosin light chain phosphorylation. Mol Biol Cell. 2017; 28:3832–3843. [PubMed: 29046396]

Katono K, Sato Y, Jiang SX, Kobayashi M, Nagashio R, Ryuge S, Fukuda E, Goshima N, Satoh Y, Saegusa M, Masuda N. Prognostic significance of MYH9 expression in resected non-small cell lung cancer. PLoS One. 2015; 10:e0121460. [PubMed: 25826333]

Kaushansky K. Thrombopoiesis. Semin Hematol. 2015; 52:4–11. [PubMed: 25578413]

Kawamoto S, Bengur AR, Sellers JR, Adelstein RS. In situ phosphorylation of human platelet myosin heavy and light chains by protein kinase C. J Biol Chem. 1989; 264:2258–2265. [PubMed: 2914906]

Kawamoto S, Adelstein RS. Chicken nonmuscle myosin heavy chains: differential expression of two mRNAs and evidence for two different polypeptides. J Cell Biol. 1991; 112:915–924. [PubMed: 1999462]

Kelley MJ, Jawien W, Ortel TL, Korczak JF. Mutation of MYH9, encoding non-muscle myosin heavy chain A, in May-Hegglin anomaly. Nat Genet. 2000; 26:106–108. [PubMed: 10973260]

Kim KY, Kovacs m, Kawamoto S, Sellers JR, Adelstein RS. Disease-associated mutations and alternative splicing alter the enzymatic and motile activity of nonmuscle myosins II-B and II-C. J Biol Chem. 2005; 280:22769–22775. [PubMed: 15845534]

Kim SJ, Lee S, Park HJ, Kang TH, Sagong B, Baek JI, Oh SK, Choi JY, Lee KY, Kim UK. Genetic association of MYH genes with hereditary hearing loss in Korea. Gene. 2016; 591:177–182. [PubMed: 27393652]

Kiss B, Duelli A, Radnai L, Kekesi KA, Katona G, Nyitray L. Crystal structure of the S100A4-nonmuscle myosin IIA tail fragment complex reveals an asymmetric target binding mechanism. Proc Natl Acad Sci U S A. 2012; 109:6048–6053. [PubMed: 22460785]

Kitamura K, Yoshida K, Shiraishi Y, Chiba K, Tanaka H, Furukawa K, Miyano S, Ogawa S, Kunishima S. Normal neutrophil myosin IIA localization in an immunofluorescence analysis can rule out MYH9 disorders. J Thromb Haemost. 2013; 11:2071–2073. [PubMed: 24106837]

Komatsu S, Ikebe M. The phosphorylation of myosin II at the Ser1 and Ser2 is critical for normal platelet-derived growth factor induced reorganization of myosin filaments. Mol Biol Cell. 2007; 18:5081–5090. [PubMed: 17928407]

Kopp JB, Smith MW, Nelson GW, Johnson RC, Freedman BI, Bowden DW, Oleksyk T, McKenzie LM, Kajiyama H, Ahuja TS, Berns JS, Briggs W, Cho ME, Dart RA, Kimmel PL, Korbet SM, Michel DM, Mokrzycki MH, Schelling JR, Simon E, Trachtman H, Vlahov D, Winkler CA. MYH9 is a major-effect risk gene for focal segmental glomerulosclerosis. Nat Genet. 2008; 40:1175–1184. [PubMed: 18794856]

Kopp JB. Glomerular pathology in autosomal dominant MYH9 spectrum disorders: what are the clues telling us about disease mechanism? Kidney Int. 2010; 78:130–133. [PubMed: 20588287]

Kopp JB, Nelson GW, Sampath K, Johnson RC, Genovese G, An P, Friedman D, Briggs W, Dart R, Korbet S, Mokrzycki MH, Kimmel PL, Limou S, Ahuja TS, Berns JS, Fryc J, Simon EE, Smith MC, Trachtman H, Michel DM, Schelling JR, Vlahov D, Pollak M, Winkler CA. APOL1 genetic

variants in focal segmental glomerulosclerosis and HIV-associated nephropathy. J Am Soc Nephrol. 2011; 22:2129–2137. [PubMed: 21997394]

Kunishima S, Kojima T, Matsushita T, Tanaka T, Tsurusawa M, Furukawa Y, Nakamura Y, Okamura T, Amemiya N, Nakayama T, Kamiya T, Saito H. Mutations in the NMMHC-A gene cause autosomal dominant macrothrombocytopenia with leukocyte inclusions (May-Hegglin anomaly/Sebastian syndrome). Blood. 2001; 97:1147–1149. [PubMed: 11159552]

Kunishima S, Matsushita T, Kojima T, Sako M, Kimura F, Jo EK, Inoue C, Kamiya T, Saito H. Immunofluorescence analysis of neutrophil nonmuscle myosin heavy chain-A in MYH9 disorders: association of subcellular localization with MYH9 mutations. Lab Invest. 2003; 83:115–122. [PubMed: 12533692]

Kunishima S, Matsushita T, Yoshihara T, Nakase Y, Yokoi K, Hamaguchi M, Saito H. First description of somatic mosaicism in MYH9 disorders. Br J Haematol. 2005; 128:360–365. [PubMed: 15667538]

Kunishima S, Yoshinari M, Nishio H, Ida K, Miura T, Matsushita T, Hamaguchi M, Saito H. Haematological characteristics of MYH9 disorders due to MYH9 R702 mutations. Eur J Haematol. 2007; 78:220–226. [PubMed: 17241369]

Kunishima S, Takaki K, Ito Y, Saito H. Germinal mosaicism in MYH9 disorders: a family with two affected siblings of normal parents. Br J Haematol. 2009; 145:260–262. [PubMed: 19208103]

Kunishima S, Kitamura K, Matsumoto T, Sekine T, Saito H. Somatic mosaicism in MYH9 disorders: the need to carefully evaluate apparently healthy parents. Br J Haematol. 2014; 165:885–887. [PubMed: 24611568]

Lalwani AK, Goldstein JA, Kelley MJ, Luxford W, Castelein CM, Mhatre AN. Human nonsyndromic hereditary deafness DFNA17 is due to a mutation in nonmuscle myosin MYH9. Am J Hum Genet. 2000; 67:1121–1128. [PubMed: 11023810]

Larson MK, Watson SP. A product of their environment: do megakaryocytes rely on extracellular cues for proplatelet formation? Platelets. 2006; 17:435–440. [PubMed: 17074718]

Li ZH, Bresnick AR. The S100A4 metastasis factor regulates cellular motility via a direct interaction with myosin-IIA. Cancer Res. 2006; 66:5173–5180. [PubMed: 16707441]

Li ZH, Dulyaninova NG, House RP, Almo SC, Bresnick AR. S100A4 regulates macrophage chemotaxis. Mol Biol Cell. 2010; 21:2598–2610. [PubMed: 20519440]

Liao Q, Li R, Zhou R, Pan Z, Xu L, Ding Y, Zhao L. LIM kinase 1 interacts with myosin-9 and alpha-actinin-4 and promotes colorectal cancer progression. Br J Cancer. 2017; 117:563–571. [PubMed: 28664914]

Lin ZH, Zhen YY, Chien KY, Lee IC, Lin WC, Chen MY, Pai LM. LIMCH1 regulates nonmuscle myosin-II activity and suppresses cell migration. Mol Biol Cell. 2017; 28:1054–1065. [PubMed: 28228547]

Ludowyke RI, Elgundi Z, Kranenburg T, Stehn JR, Schmitz-Peiffer C, Hughes WE, Biden TJ. Phosphorylation of nonmuscle myosin heavy chain IIA on Ser1917 is mediated by protein kinase C beta II and coincides with the onset of stimulated degranulation of RBL-2H3 mast cells. J Immunol. 2006; 177:1492–1499. [PubMed: 16849455]

Ma X, Jana SS, Conti MA, Kawamoto S, Claycomb WC, Adelstein RS. Ablation of nonmuscle myosin II-B and II-C reveals a role for nonmuscle myosin II in cardiac myocyte karyokinesis. Mol Biol Cell. 2010; 21:3952–3962. [PubMed: 20861308]

Ma X, Adelstein RS. In vivo studies on nonmuscle myosin II expression and function in heart development. Front Biosci (Landmark Ed). 2012; 17:545–555. [PubMed: 22201759]

Ma X, Adelstein RS. The role of vertebrate nonmuscle Myosin II in development and human disease. Bioarchitecture. 2014; 4:88–102. [PubMed: 25098841]

Marigo V, Nigro A, Pecci A, Montanaro D, Di Stazio M, Balduini CL, Savoia A. Correlation between the clinical phenotype of *MYH9*-related disease and tissue distribution of class II non-muscle myosin heavy chains. Genomics. 2004; 83:1125–1133. [PubMed: 15177565]

Milton DL, Schneck AN, Ziech DA, Ba M, Facemyer KC, Halayko AJ, Baker JE, Gerthoffer WT, Cremo CR. Direct evidence for functional smooth muscle myosin II in the 10S self-inhibited monomeric conformation in airway smooth muscle cells. Proc Natl Acad Sci U S A. 2011; 108:1421–1426. [PubMed: 21205888]

Miyagawa M, Naito T, Nishio SY, Kamatani N, Usami S. Targeted exon sequencing successfully discovers rare causative genes and clarifies the molecular epidemiology of Japanese deafness patients. PLoS One. 2013; 8:e71381. [PubMed: 23967202]

Miyazaki K, Kunishima S, Fujii W, Higashihara M. Identification of three in-frame deletion mutations in MYH9 disorders suggesting an important hot spot for small rearrangements in MYH9 exon 24. Eur J Haematol. 2009; 83:230–234. [PubMed: 19459928]

Moussavi RS, Kelley CA, Adelstein RS. Phosphorylation of vertebrate nonmuscle and smooth muscle myosin heavy chains and light chains. Mol Cell Biochem. 1993; 127–128:219–227.

Neveling K, Feenstra I, Gilissen C, Hoefsloot LH, Kamsteeg EJ, Mensenkamp AR, Rodenburg RJ, Yntema HG, Spruijt L, Vermeer S, Rinne T, van Gassen KL, Bodmer D, Lugtenberg D, de Reuver R, Buijsman W, Derks RC, Wieskamp N, van den Heuvel B, Ligtenberg MJ, Kremer H, Koolen DA, van de Warrenburg BP, Cremers FP, Marcelis CL, Smeitink JA, Wortmann SB, van Zelst-Stams WA, Veltman JA, Brunner HG, Scheffer H, Nelen MR. A post-hoc comparison of the utility of sanger sequencing and exome sequencing for the diagnosis of heterogeneous diseases. Hum Mutat. 2013; 34:1721–1726. [PubMed: 24123792]

Nishikawa M, Sellers JR, Adelstein RS, Hidaka H. Protein kinase C modulates in vitro phosphorylation of the smooth muscle heavy meromyosin by myosin light chain kinase. J Biol Chem. 1984; 259:8808–8814. [PubMed: 6235218]

Noris P, Klersy C, Gresele P, Giona F, Giordano P, Minuz P, Loffredo G, Pecci A, Melazzini F, Civaschi E, Mezzasoma A, Piedimonte M, Semeraro F, Veneri D, Menna F, Ciardelli L, Balduini CL. Italian Gruppo di Studio delle Piastrine. Platelet size for distinguishing between inherited thrombocytopenias and immune thrombocytopenia: a multicentric, real life study. Br J Haematol. 2013; 162:112–119. [PubMed: 23617394]

Noris P, Biino G, Pecci A, Civaschi E, Savoia A, Seri M, Melazzini F, Loffredo G, Russo G, Bozzi V, Notarangelo LD, Gresele P, Heller PG, Pujol-Moix N, Kunishima S, Cattaneo M, Bussel J, De Candia E, Cagioni C, Ramenghi U, Barozzi S, Fabris F, Balduini CL. Platelet diameters in inherited thrombocytopenias: analysis of 376 patients with all known disorders. Blood. 2014; 124:e4–e10. [PubMed: 24990887]

Odronitz F, Kollmar M. Drawing the tree of eukaryotic life based on the analysis of. 2007; 2:269 m. anually annotated myosins from 328 species. Genome Biol, 8, R196.

O'Seaghdha CM, Parekh RS, Hwang SJ, Li M, Köttgen A, Coresh J, Yang Q, Fox CS, Kao WH. The MYH9/APOL1 region and chronic kidney disease in European-Americans. Hum Mol Genet. 2011; 20:2450–2456. [PubMed: 21429915]

Pecci A, Panza E, Pujol-Moix N, Klersy C, Di Bari F, Bozzi V, Gresele P, Lethagen S, Fabris F, Dufour C, Granata A, Doubek M, Pecoraro C, Koivisto PA, Heller PG, Iolascon A, Alvisi P, Schwabe D, De Candia E, Rocca B, Russo U, Ramenghi U, Noris P, Seri M, Balduini CL, Savoia A. Position of nonmuscle myosin heavy chain IIA (NMMHC-IIA) mutations predicts the natural history of MYH9-related disease. Hum Mutat. 2008a; 29:409–417. [PubMed: 18059020]

Pecci A, Granata A, Fiore CE, Balduini CL. Renin-angiotensin system blockade is effective in reducing proteinuria of patients with progressive nephropathy caused by MYH9 mutations (Fechtner-Epstein syndrome). Nephrol Dial Transplant. 2008b; 23:2690–2692. [PubMed: 18503011]

Pecci A, Malara A, Badalucco S, Bozzi V, Torti M, Balduini CL, Balduini A. Megakaryocytes of patients with MYH9-related thrombocytopenia present an altered proplatelet formation. Thromb Haemost. 2009; 102:90–96. [PubMed: 19572073]

Pecci A, Gresele P, Klersy C, Savoia A, Noris P, Fierro T, Bozzi V, Mezzasoma AM, Melazzini F, Balduini CL. Eltrombopag for the treatment of the inherited thrombocytopenia deriving from MYH9 mutations. Blood. 2010; 116:5832–5837. [PubMed: 20844233]

Pecci A, Bozzi V, Panza E, Barozzi S, Gruppi C, Seri M, Balduini CL. Mutations responsible for MYH9-related thrombocytopenia impair SDF-1-driven migration of megakaryoblastic cells. Thromb Haemost. 2011; 106:693–704. [PubMed: 21833445]

Pecci A, Biino G, Fierro T, Bozzi V, Mezzasoma A, Noris P, Ramenghi U, Loffredo G, Fabris F, Momi S, Magrini U, Pirastu M, Savoia A, Balduini C, Gresele P. Italian Registry for MYH9-releated diseases. Alteration of liver enzymes is a feature of the MYH9-related disease syndrome. PLoS One. 2012a; 7:e35986. [PubMed: 22558294]

Pecci A, Barozzi S, d'Amico S, Balduini CL. Short-term eltrombopag for surgical preparation of a patient with inherited thrombocytopenia deriving from MYH9 mutation. Thromb Haemost. 2012b; 107:1188–1189. [PubMed: 22398565]

Pecci A, Klersy C, Gresele P, Lee KJ, De Rocco D, Bozzi V, Russo G, Heller PG, Loffredo G, Ballmaier M, Fabris F, Beggiato E, Kahr WH, Pujol-Moix N, Platokouki H, Van Geet C, Noris P, Yerram P, Hermans C, Gerber B, Economou M, De Groot M, Zieger B, De Candia E, Fraticelli V, Kersseboom R, Piccoli GB, Zimmermann S, Fierro T, Glembotsky AC, Vianello F, Zaninetti C, Nicchia E, Güthner C, Baronci C, Seri M, Knight PJ, Balduini CL, Savoia A. MYH9-related disease: a novel prognostic model to predict the clinical evolution of the disease based on genotype-phenotype correlations. Hum Mutat. 2014a; 35:236–247. [PubMed: 24186861]

Pecci A, Verver EJ, Schlegel N, Canzi P, Boccio CM, Platokouki H, Krause E, Benazzo M, Topsakal V, Greinacher A. Cochlear implantation is safe and effective in patients with MYH9-related disease. Orphanet J Rare Dis. 2014b; 9:100. [PubMed: 24980457]

Peterson LC, Rao KV, Crosson JT, White JG. Fechtner syndrome--a variant of Alport's syndrome with leukocyte inclusions and macrothrombocytopenia. Blood. 1985; 65:397–406. [PubMed: 2981587]

Raab M, Swift J, Dingal PC, Shah P, Shin JW, Discher DE. Crawling from soft to stiff matrix polarizes the cytoskeleton and phosphoregulates myosin-II heavy chain. J Cell Biol. 2012; 199:669–683. [PubMed: 23128239]

Rai V, Thomas DG, Beach JR, Egelhoff TT. Myosin IIA Heavy Chain Phosphorylation Mediates Adhesion Maturation and Protrusion in Three Dimensions. J Biol Chem. 2017; 292:3099–3111. [PubMed: 28053086]

Ramagopal UA, Dulyaninova NG, Varney KM, Wilder PT, Nallamsetty S, Brenowitz M, Weber DJ, Almo SC, Bresnick AR. Structure of the S100A4/myosin-IIA complex. BMC Struct Biol. 2013; 13:31. [PubMed: 24252706]

Ravid S. The tumor suppressor Lgl1 regulates front-rear polarity of migrating cells. Cell Adh Migr. 2014; 8:378–383. [PubMed: 25482644]

Rocca B, Laghi F, Zini G, Maggiano N, Landolfi R. Fechtner syndrome: report of a third family and literature review. Br J Haematol. 1993; 85:423–426. [PubMed: 8280620]

Sandquist JC, Means AR. The C-terminal tail region of nonmuscle myosin II directs isoform-specific distribution in migrating cells. Mol Biol Cell. 2008; 19:5156–5167. [PubMed: 18843042]

Saposnik B, Binard S, Fenneteau O, Nurden A, Nurden P, Hurtaud-Roux MF, Schlegel N. French MYH9 network. Mutation spectrum and genotype-phenotype correlations in a large French cohort of MYH9-Related Disorders. Mol Genet Genomic Med. 2014; 2:297–312. [PubMed: 25077172]

Savoia, A., Pecci, A. [updated 2015 Jul 16] MYH9-Related Disorders. In: Pagon, RA.Adam, MP.Ardinger, HH.Wallace, SE.Amemiya, A.Bean, LJH.Bird, TD.Ledbetter, N.Mefford, HC.Smith, RJH., Stephens, K., editors. GeneReviews® [Internet]. Seattle (WA): University of Washington, Seattle; 2008. p. 1993-2017.Available from http://www.ncbi.nlm.nih.gov/books/NBK2689/PubMedPMID:20301740

Savoia A, De Rocco D, Panza E, Bozzi V, Scandellari R, Loffredo G, Mumford A, Heller PG, Noris P, De Groot MR, Giani M, Freddi P, Scognamiglio F, Riondino S, Pujol-Moix N, Fabris F, Seri M, Balduini CL, Pecci A. Heavy chain myosin 9-related disease (MYH9 -RD): neutrophil inclusions of myosin-9 as a pathognomonic sign of the disorder. Thromb Haemost. 2010; 103:826–832. [PubMed: 20174760]

Schramek D, Sendoel A, Segal JP, Beronja S, Heller E, Oristian D, Reva B, Fuchs E. Direct in vivo RNAi screen unveils myosin IIa as a tumor suppressor of squamous cell carcinomas. Science. 2014; 343:309–313. [PubMed: 24436421]

Sebé-Pedrós A, Grau-Bové X, Richards TA, Ruiz-Trillo I. Evolution and classification of myosins, a paneukaryotic whole-genome approach. Genome Biol Evol. 2014; 6:290–305. [PubMed: 24443438]

Sekine T, Konno M, Sasaki S, Moritani S, Miura T, Wong WS, Nishio H, Nishiguchi T, Ohuchi MY, Tsuchiya S, Matsuyama T, Kanegane H, Ida K, Miura K, Harita Y, Hattori M, Horita S, Igarashi T, Saito H, Kunishima S. Patients with Epstein-Fechtner syndromes owing to MYH9 R702

mutations develop progressive proteinuric renal disease. Kidney Int. 2010; 78:207–214. [PubMed: 20200500]

Sellers JR, Pato MD, Adelstein RS. Reversible phosphorylation of smooth muscle myosin, heavy meromyosin, and platelet myosin. J Biol Chem. 1981; 256:13137–13142. [PubMed: 6118372]

Sellers JR. Myosins: a diverse superfamily. Biochim Biophys Acta, 2000. 2000; 1496:3–22.

Seri M, Cusano R, Gangarossa S, Caridi G, Bordo D, Lo Nigro C, Ghiggeri GM, Ravazzolo R, Savino M, Del Vecchio M, d'Apolito M, Iolascon A, Zelante LL, Savoia A, Balduini CL, Noris P, Magrini U, Belletti S, Heath KE, Babcock M, Glucksman MJ, Aliprandis E, Bizzaro N, Desnick RJ, Martignetti JA. Mutations in MYH9 result in the May-Hegglin anomaly, and Fechtner and Sebastian syndromes. The May-Heggllin/Fechtner Syndrome Consortium. Nat Genet. 2000; 26:103–105. [PubMed: 10973259]

Seri M, Pecci A, Di Bari F, Cusano R, Savino M, Panza E, Nigro A, Noris P, Gangarossa S, Rocca B, Gresele P, Bizzaro N, Malatesta P, Koivisto PA, Longo I, Musso R, Pecoraro C, Iolascon A, Magrini U, Rodriguez Soriano J, Renieri A, Ghiggeri GM, Ravazzolo R, Balduini CL, Savoia A. MYH9-related disease: May-Hegglin anomaly, Sebastian syndrome, Fechtner syndrome, and Epstein syndrome are not distinct entities but represent a variable expression of a single illness. Medicine (Baltimore). 2003; 82:203–215. [PubMed: 12792306]

Shutova MS, Spessott WA, Giraudo CG, Svitkina T. Endogenous species of mammalian nonmuscle myosin IIA and IIB include activated monomers and heteropolymers. Curr Biol. 2014; 24:1958–1968. [PubMed: 25131674]

Shutova MS, Asokan SB, Talwar S, Assoian RK, Bear JE, Svitkina TM. Self-sorting of nonmuscle myosins IIA and IIB polarizes the cytoskeleton and modulates cell motility. J Cell Biol. 2017; 216:2877–2889. [PubMed: 28701425]

Sloan-Heggen CM, Bierer AO, Shearer AE, Kolbe DL, Nishimura CJ, Frees KL, Ephraim SS, Shibata SB, Booth KT, Campbell CA, Ranum PT, Weaver AE, Black-Ziegelbein EA, Wang D, Azaiez H, Smith RJ. Comprehensive genetic testing in the clinical evaluation of 1119 patients with hearing loss. Hum Genet. 2016; 135:441–450. [PubMed: 26969326]

Suzuki N, Kunishima S, Ikejiri M, Maruyama S, Sone M, Takagi A, Ikawa M, Okabe M, Kojima T, Saito H, Naoe T, Matsushita T. Establishment of mouse model of MYH9 disorders: heterozygous R702C mutation provokes macrothrombocytopenia with leukocyte inclusion bodies, renal glomerulosclerosis and hearing disability. PLoS One. 2013; 8:e71187. [PubMed: 23976996]

Takeda K, Kishi H, Ma X, Yu ZX, Adelstein RS. Ablation and mutation of nonmuscle myosin heavy chain II-B results in a defect in cardiac myocyte cytokinesis. Circ Res. 2003; 93:330–337. [PubMed: 12893741]

Thon JN, Italiano JE. Platelets: production, morphology and ultrastructure. Handbook of Experimental Pharmacology. 2012a; 210:3–22.

Thon JN, Italiano JE Jr. Does size matter in platelet production? Blood. 2012b; 120:1552–1561. [PubMed: 22665937]

Thon JN, Macleod H, Begonja AJ, Zhu J, Lee KC, Mogilner A, Hartwig JH, Italiano JE Jr. Microtubule and cortical forces determine platelet size during vascular platelet production. Nature Communications. 2012; 3:852.

Totsukawa G, Yamakita Y, Yamashiro S, Hartshorne DJ, Sasaki Y, Matsumura F. Distinct roles of ROCK (Rho-kinase) and MLCK in spatial regulation of MLC phosphorylation for assembly of stress fibers and focal adhesions in 3T3 fibroblasts. J Cell Biol. 2000; 150:797–806. [PubMed: 10953004]

Tzur S, Rosset S, Shemer R, Yudkovsky G, Selig S, Tarekegn A, Bekele E, Bradman N, Wasser WG, Behar DM, Skorecki K. Missense mutations in the APOL1 gene are highly associated with end stage kidney disease risk previously attributed to the MYH9 gene. Hum Genet. 2010; 128:345–350. [PubMed: 20635188]

Verver E, Pecci A, De Rocco D, Ryhänen S, Barozzi S, Kunst H, Topsakal V, Savoia A. R705H mutation of MYH9 is associated with MYH9-related disease and not only with non-syndromic deafness DFNA17. Clin Genet. 2015; 88:85–89. [PubMed: 24890873]

Verver EJ, Topsakal V, Kunst HP, Huygen PL, Heller PG, Pujol-Moix N, Savoia A, Benazzo M, Fierro T, Grolman W, Gresele P, Pecci A. Nonmuscle Myosin Heavy Chain IIA Mutation Predicts

Severity and Progression of Sensorineural Hearing Loss in Patients With MYH9-Related Disease. Ear Hear. 2016; 37:112–120. [PubMed: 26226608]

Vicente-Manzanares M, Ma X, Adelstein RS, Horwitz AR. Non-muscle myosin II takes centre stage in cell adhesion and migration. Nat Rev Mol Cell Biol. 2009; 10:778–790. [PubMed: 19851336]

Wang A, Ma X, Conti MA, Liu C, Kawamoto S, Adelstein RS. Nonmuscle myosin II isoform and domain specificity during early mouse development. Proc Natl Acad Sci U S A. 2010; 107:14645–14650. [PubMed: 20679233]

Wendt T, Taylor D, Messier T, Trybus KM, Taylor KA. Visualization of head-head interactions in the inhibited state of smooth muscle myosin. J Cell Biol. 1999; 147:1385–1390. [PubMed: 10613897]

Wu CC, Lin YH, Lu YC, Chen PJ, Yang WS, Hsu CJ, Chen PL. Application of massively parallel sequencing to genetic diagnosis in multiplex families with idiopathic sensorineural hearing impairment. PLoS One. 2013; 8:e57369. [PubMed: 23451214]

Yamanouchi J, Hato T, Kunishima S, Niiya T, Nakamura H, Yasukawa M. A novel MYH9 mutation in a patient with MYH9 disorders and platelet size-specific effect of romiplostim on macrothrombocytopenia. Ann Hematol. 2015; 94:1599–1600. [PubMed: 26051904]

Ye G, Huang K, Yu J, Zhao L, Zhu X, Yang Q, Li W, Jiang Y, Zhuang B, Liu H, Shen Z, Wang D, Yan L, Zhang L, Zhou H, Hu Y, Deng H, Liu H, Li G, Qi X. MicroRNA-647 Targets SRF-MYH9 Axis to Suppress Invasion and Metastasis of Gastric Cancer. Theranostics. 2017; 7:3338–3353. [PubMed: 28900514]

Zhang Y, Conti MA, Malide D, Dong F, Wang A, Shmist YA, Liu C, Zerfas P, Daniels MP, Chan CC, Kozin E, Kachar B, Kelley MJ, Kopp JB, Adelstein RS. Mouse models of MYH9-related disease: mutations in nonmuscle myosin II-A. Blood. 2012; 119:238–250. [PubMed: 21908426]

Zhu T, He Y, Yang J, Fu W, Xu X, Si Y. MYBPH inhibits vascular smooth muscle cell migration and attenuates neointimal hyperplasia in a rat carotid balloon-injury model. Exp Cell Res. 2017; 359:154–162. [PubMed: 28800959]

HIGHLIGHTS

- The *MYH9* genes encodes the heavy chain of the non-muscle myosin IIA (NM IIA), a cytoplasmic myosin expressed in most cells and tissues.
- NM IIA participates in several processes requiring the generation of intracellular chemomechanical force and translocation of the actin cytoskeleton.
- NM IIA functions are finely regulated by phosphorylation of its 20kDa light chain, of the heavy chain, and by interactions with a variety of other proteins.
- Mutations in *MYH9* cause a syndromic autosomal-dominant disorder, termed *MYH9*-related disease.
- *MYH9* variants may also be involved in other human diseases, such as cancer, chronic kidney disease, and non-syndromic deafness.

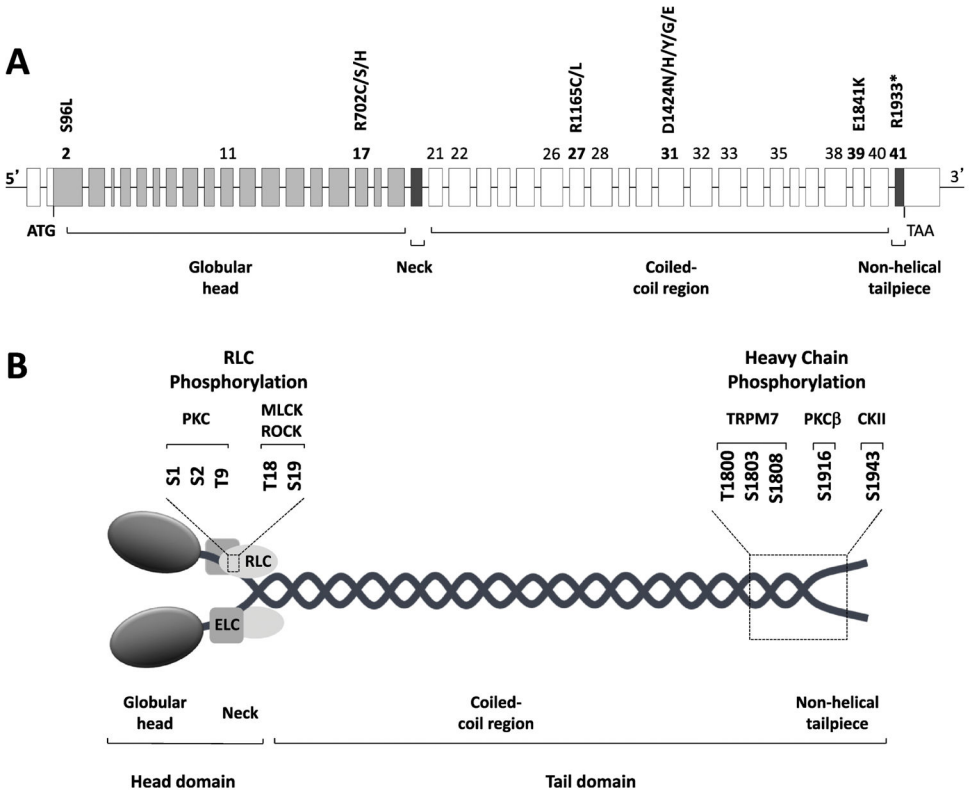

Figure 1. MYH9 gene and protein organization

(A): Genomic structure of the *MYH9* gene. *MYH9* spans more than 106 kbp on chromosome 22q12.3 and is composed of 41 exons. The open reading frame spans exon 2 to exon 41 and encodes the non-muscle myosin heavy chain IIA, a protein of 1,960 amino acids. The numbers of the exons affected by the almost 90 different mutations responsible for *MYH9*-related disease (listed in Table 2) are indicated. Exons where hot spots of mutations are located, as well as the most frequent mutations, which account for approximately 70% of the *MYH9*-related disease families, are indicated in bold. (B): Schematic representation of non-muscle myosin IIA (NM IIA). NM IIA is a hexameric molecule consisting of a dimer of heavy chains, two regulatory light chains (RLC) and two essential light chains (ELC). Each heavy chain comprises the N-terminal head domain, which includes the motor (globular head, encoded by exons 1–19 of *MYH9*) and the neck (exon 20), and the C-terminal tail domain. The tail domain includes the long coiled-coil region (exons 21–40) and the short non-helical tailpiece (exon 41). Serine and threonine residues of RLC and heavy chains involved in phosphorylation, as well as the specific kinases, are indicated. PKC, protein kinase C; MLCK, myosin light chain kinase; ROCK, Rho-associated protein kinase; TRPM7, transient receptor potential melastatin 7; PKCβ, protein kinase Cβ; CKII, casein kinase II.

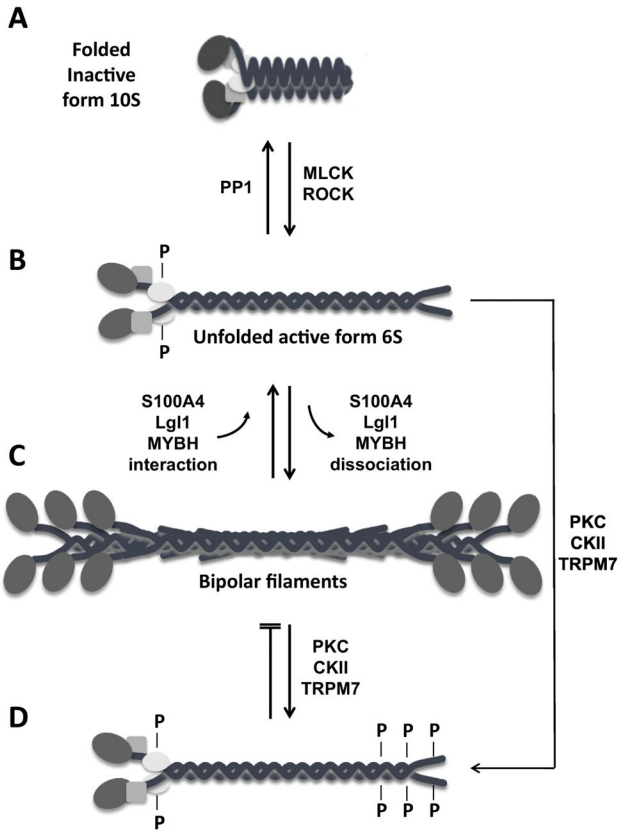

Figure 2. Regulation of non-muscle myosin IIA filament assembly

(A): Diagram of the folded, inactive 10S form of non-muscle myosin IIA (NM IIA) which is unable to assembly into filaments. Myosin light chain kinase (MLCK) and Rho-associated protein kinase (ROCK) phosphorylate RLC on serine 19 and threonine 18, allowing NM IIA to assume an unfolded active 6S conformation (B) and to assemble into bipolar filaments (C). The only known phosphatase that removes the phosphate group from these residues is protein phosphatase 1 (PP1). Assembly and disassembly of the bipolar filaments is also regulated by the interaction of NM IIA with S100A4, Lethal giant larvae (Lgl1), or myosin binding protein H (MYBH). (D) Phosphorylation of residues at the C-terminus of NM IIA by different kinases, such as protein kinase C (PKC), casein kinase 2 (CKII), and transient receptor potential melastatin 7 (TRPM7), either disassemblies the bipolar filaments or prevents their formation.

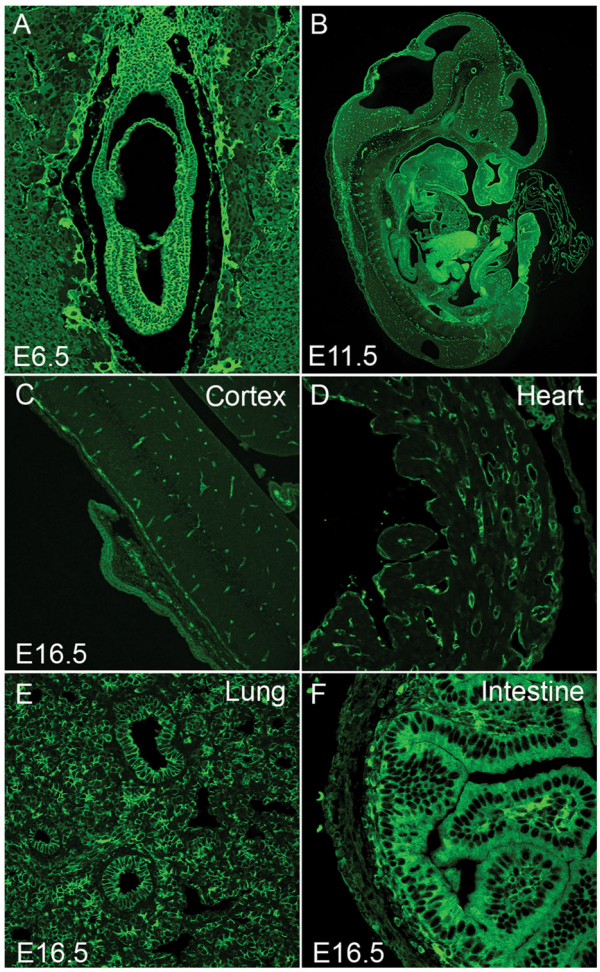

Figure 3. Expression of NM IIA in Developing Mouse Embryos

Sections of paraformaldehyde-fixed mouse embryos were stained with antibodies to NMHC IIA (green). NM IIA is widely distributed throughout the mouse embryos at E6.5 (A) and E11.5 (B). In E6.5 embryos, NM IIA is detected in all cells with similar staining intensity in both embryonic and extra-embryonic tissues (A). In E11.5 mouse embryos, different tissues and cells show marked variation in their staining intensity (B). In E16.5 mouse embryos, NM II-A is enriched in vasculature (endothelial cells) in brain (C), non-myocytes in heart (D), epithelial as well as interstitial mesenchymal cells in lung (E), and epithelial cells in intestine (F).

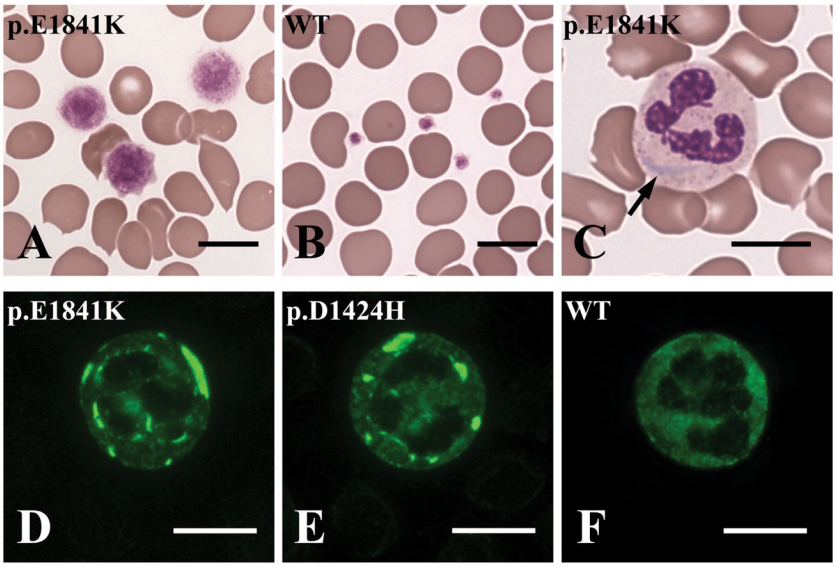

Figure 4. Abnormalities detectable at the examination of peripheral blood smears in patients with *MYH9*-related disease (*MYH9*-RD)

(A–C): Conventional panoptical May-Grünwald-Giemsa staining. (D–F): Immunofluorescence staining for the MYH9 protein (NMHC IIA). (A): Platelets of *MYH9*-RD patients are characterized by an extreme degree of macrocytosis: some platelets are even larger than erythrocytes (giant platelets). In (B) platelets of a healthy subjects are shown for comparison. (C): Aggregates of the MYH9 protein in the cytoplasm of neutrophil granulocytes may be identified after conventional staining of blood smears as faint basophilic (sky-blue) inclusion bodies, called “Döhle-like” bodies (arrow). (D–E): Immunofluorescence staining with antibodies to NMHC IIA allows to clearly detect the typical NMHC IIA aggregates in the cytoplasm of granulocytes of *MYH9*-RD patients and a definite diagnosis of the disorder. In (F) the distribution of the MYH9 protein in a granulocyte of a healthy individual is shown for comparison. The MYH9 genotypes of each individual are indicated in each image. WT, wild type. Scale bars correspond to 10 μm.

Table 1

Mass Spectroscopy Analysis of the Relative Abundance of Nonmuscle Myosin II Heavy Chain Isoforms in Mouse Tissues, Human Platelets and Cell Lines

Tissues/Cell Lines	NMHC II-A	NMHC II-B	NMHC II-C	N (of samples)
Mouse Heart (P2)	63±3%	37±3%	ND	2
Mouse Heart (adult)	96±4%	5±3%	ND	2
Mouse Cerebral Cortex	29±9%	67±13%	4±8%	3
Mouse Cerebellum	14±16%	81±19%	6±5%	4
Mouse Spinal Cord	29±9%	65±5%	6±9%	5
Mouse Kidney	92±4%	7±1%	2±2%	2
Mouse Lung	41±2%	22±1%	37±4%	2
Mouse Spleen	100%	ND	ND	2
Mouse ES Cells	81±7%	19±7%	ND	4
Human Platelets	100%	ND	ND	3
3T3 Cells (ms)	83±7%	17±7%	ND	3
Caco2-BBE Cells (hu)	89±4%	5±2%	6±2%	2
COS-7 Cells (mk)	ND	86±19%	15±19%	2
HeLa Cells (hu)	97±3%	3±3%	ND	4
HFF Cells (hu)	95±4%	4±4%	1±1%	5
HL-1 Cells (ms)	95±3%	5±3%	ND	3
HT29 Cells (hu)	54±3%	1±1%	45±3%	4
MDCK Cells (dog)	96±3%	1±1%	3±2%	2
RBL Cells (rat)	99±1%	1±1%	1±2%	4

ND, not detected; P2, postnatal day 2; HFF, human foreskin fibroblasts; ms, mouse, hu, human; mk, monkey.

Table 2

Mutations identified in the *MYH9* gene and associated with *MYH9*-related disease.

Exon	DNA[a]	Protein[b]	References[c]
2	c.97T>A	p.**Trp33**Arg	Jang et al., 2012
	c.97T>C		Sun et al., 2012
	c.99G>C	p.**Trp33**Cys	Saposnik et al., 2014
	c.99G>T		Balduini et al., 2011
	c.99_103delinsTGTGG	p.**Trp33**_Pro35delinsCysValAla	Miyajima et al., 2009
	c.101T>A	p.**Val34**Glu	Saposnik et al., 2014
	c.101T>G	p.**Val34**Gly	De Rocco et al., 2013
	c.121T>C	p.Phe41Leu	Yoshimi et al., 2016
	c.130G>C	p.Ala44Pro	Saposnik et al., 2014
	c.220A>G	p.Lys74Glu	Kanematsu et al., 2016
	c.228_245del	p.Asn76_Ser81del	Balduini et al., 2011
	c.277A>G	p.**Asn93**Asp	Saposnik et al., 2014
	c.279C>G	p.**Asn93**Lys	Balduini et al., 2011
	c.283G>A	p.**Ala95**Thr	Balduini et al., 2011
	c.284C>A	p.**Ala95**Asp	Balduini et al., 2011
	c.284C>T	p.**Ala95**Val	Saposnik et al., 2014
	c.287C>T	p.Ser96Leu	Balduini et al., 2011
11	c.1115A>G	p.Gln372Arg	Saposnik et al., 2014
	c.1119G>C	p.Lys373Asn	Balduini et al., 2011
17	c.2104C>T	p.**Arg702**Cys	Balduini et al., 2011
	c.2104C>A	p.**Arg702**Ser	De Rocco et al., 2013
	c.2105G>A	p.**Arg702**His	Balduini et al., 2011
	c.2114G>A	p.Arg705His	Balduini et al., 2011
	c.2116C>G	p.Gln706Glu	Balduini et al., 2011
	c.2152C>T	p.Arg718Trp	Balduini et al., 2011
21	c.2539_2559dup	p.Met847_Glu853dup	Glembotsky et al., 2012
	c.2548A>G	p.Lys850Glu	Saposnik et al., 2014
22	c.2680G>A	p.Glu894Lys	Saposnik et al., 2014
	c.3142_3162del	p.Lys1048_Glu1054del	De Rocco et al., 2013
	c.3164_3205del	p.Gly1055_Gln1068del	Balduini et al., 2011
	c.3195_3215del	p.Glu1066_Ala1072del	Balduini et al., 2011
	c.3195_3215dup	p.Glu1066_Ala1072dup	Balduini et al., 2011
	c.3202_3222del	p.Gln1068_Leu1074del	Ishida et al., 2013
	c.3250_3252del	p.Glu1084del	Balduini et al., 2011
26	1220 kb del	p.Val1092_Arg1162del	Balduini et al., 2011
	c.3340T>C	p.Ser1114Pro	Balduini et al., 2011

Exon	DNA[a]	Protein[b]	References[c]
	c.3463A>G	p.**Thr1155**Ala	Balduini et al., 2011
	c.3464C>T	p.**Thr1155**Ile	Balduini et al., 2011
	c.3485G>C	p.**Arg1162**Thr	Balduini et al., 2011
27	c.3486G>T	p.**Arg1162**Ser/p.Ser1163fs*1 (skipping exon 26)	Kunishima et al., 2012
	c.3493C>T	p.**Arg1165**Cys	Balduini et al., 2011
	c.3494G>T	p.**Arg1165**Leu	Balduini et al., 2011
	c.3613_3621del	p.Leu1205_Gln1207del	Balduini et al., 2011
28	c.3751G>A	p.Glu1251Lys	Balduini et al., 2011
31	c.4270G>C	p.A**sp1424**His	Balduini et al., 2011
	c.4270G>A	p.**Asp1424**Asn	Balduini et al., 2011
	c.4270G>T	p.**Asp1424**Tyr	Balduini et al., 2011
	c.4271A>G	p.**Asp1424**Gly	Saposnik et al., 2014
	c.4272C>A	p.**Asp1424**Glu	Saposnik et al., 2014
	c.4272C>G		Saposnik et al., 2014
	c.4306G>A	p.Ala1436Thr	Saposnik et al., 2014
	c.4327_4335dup	p.Gln1443_Lys1445dup	Sun et al., 2012
	c.4339G>C	p.**Asp1447**His	Balduini et al., 2011
	c.4339G>T	p.**Asp1447**Tyr	De Rocco et al., 2013
	c.4340A>T	p.**Asp1447**Val	Balduini et al., 2011
	c.4340A>G	p.**Asp1447**Gly	Schleinitz et al., 2006
32	c.4423G>A	p.Glu1475Lys	Saposnik et al., 2014
	c.4546G>C	p.**Val1516**Leu	Zhang et al., 2014
	c.4546G>T		Balduini et al., 2011
	c.4546G>A	p.**Val1516**Met	Balduini et al., 2011
33	c.4562A>G	p. His1521Arg	Ghemlas et al., 2015
	c.4670G>T	p.Arg1557Leu	Balduini et al., 2011
	c.4679T>G	p.Val1560Gly	Saposnik et al., 2014
	c.4687C>A	p.Gln1563Lys	Saposnik et al., 2014
35	c.4952T>C	p.Met1651Thr	Balduini et al., 2011
38	c.5446A>G	p.Ile1816Val	Balduini et al., 2011
39	c.5521G>A	p.Glu1841Lys	Balduini et al., 2011
40	c.5630G>A	p.Arg1877Gln	Saposnik et al., 2014
i40[d]	c.5765+2T>A	p.Arg1922Argfs*43	Saposnik et al., 2014
41	c.5770_5779del	p.Gly1924Argfs*21	Balduini et al., 2011
	c.5773del	p.Asp1925Thrfs*23	Balduini et al., 2011
	c.5774del	p.Asp1925Alafs*23	Balduini et al., 2011
	c.5780del	p.Pro1927Argfs*21	Balduini et al., 2011
	c.5788del	p.Val1930Cysfs*18	Balduini et al., 2011
	c.5794del	p.Arg1932Alafs*16	Saposnik et al., 2014

Exon	DNA[a]	Protein[b]	References[c]
	c.5797del	p.Arg1933Glufs*15	Balduini et al., 2011
	c.5797C>T	p.Arg1933*	Balduini et al., 2011
	c.5788_5793delinsCGCGGGGACCGCGGGGACCG	p.Val1930Argfs*23	Sirachainan et al., 2015
	c.5800del	p.Met1934Trpfs*14	Balduini et al., 2011
	c.5803del	p.Ala1935Profs*13	Liao et al., 2017
	c.5809A>T	p.Lys1937*	Saposnik et al., 2014
	c.5820_5821dup	p.Asp1941Glyfs*8	Saposnik et al., 2014
	c.5821del	p.Asp1941Metfs*7	Balduini et al., 2011
	c.5833G>T	p.Glu1945*	Balduini et al., 2011
	c.5842G>A	Asp1948Asn	Ali et al., 2016

[a] Nucleotide A of the ATG translation initiation start site of the *MYH9* gene cDNA in GenBank sequence NM_002473.5 is indicated as nucleotide +1.

[b] Residues affected by more than one amino acid substitutions are indicated in bold. In frame deletions/duplications/indels are in gray boxes.

[c] References reporting mutations:

- Ali S, Ghosh K, Daly ME, et al. Congenital macrothrombocytopenia is a heterogeneous disorder in India. Haemophilia 2016; 22:570–82.
- Balduini CL, Pecci A, Savoia A. Recent advances in the understanding and management of MYH9-related inherited thrombocytopenias. Br J Haematol 2011; 154:161–74.
- De Rocco D, Zieger B, Platokouki H, et al. MYH9-related disease: five novel mutations expanding the spectrum of causative mutations and confirming genotype/phenotype correlations. Eur J Med Genet 2013; 56:7–12.
- Ghemlas I, Li H, Zlateska B, et al. Improving diagnostic precision, care and syndrome definitions using comprehensive next-generation sequencing for the inherited bone marrow failure syndromes. J Med Genet 2015; 52:575–84.
- Glembotsky AC, Marta RF, Pecci A, et al. International collaboration as a tool for diagnosis of patients with inherited thrombocytopenia in the setting of a developing country. J Thromb Haemost 2012; 10:1653–61.
- Ishida M, Mori Y, Ota N, et al. Association of a novel in-frame deletion mutation of the MYH9 gene with end-stage renal failure: case report and review of the literature. Clin Nephrol 2013; 80:218–22.
- Jang MJ, Park HJ, Chong SY, et al. A Trp33Arg mutation at exon 1 of the MYH9 gene in a Korean patient with May-Hegglin anomaly. Yonsei Med J 2012; 53:662–6.
- Kanematsu T, Suzuki N, Yoshida T, et al. A case of MYH9 disorders caused by a novel mutation (p.K74E). Ann Hematol 2016; 95:161–3.
- Kunishima S, Tomii T, Kudo K, et al. G to T transversion at the first nucleotide of exon 26 of the MYH9 gene results in a novel missense mutation and abnormal splicing in platelets: comment on “A G to C transversion at the last nucleotide of exon 25 of the MYH9 gene results in a missense mutation rather than in a splicing defecton” by Vettore et al. Eur J Med Genet 2012; 55:763–5.
- Liao W, Luo X, Zhang X, et al. Genetic analysis of a pedigree affected with inherited thrombocytopenia caused by a novel mutation of MYH9 gene. Zhonghua Yi Xue Yi Chuan Xue Za Zhi 2017; 34:352–6.
- Miyajima Y, Kunishima S. Identification of the first in cis mutations in MYH9 disorder. Eur J Haematol 2009; 82:288–91.
- Saposnik B, Binard S, Fenneteau O, et al. French MYH9 network. Mutation spectrum and genotype-phenotype correlations in a large French cohort of MYH9-Related Disorders. Mol Genet Genomic Med 2014; 2: 297–312.
- Schleinitz N, Favier R, Mazodier K, et al. The MYH9 syndrome: report of a new case with a new mutation of the MYH9 gene. Rev Med Interne 2006; 27:783–6.
- Sirachainan N, Komwilaisak P, Kitamura K, et al. The first two cases of MYH9 disorders in Thailand: an international collaborative study. Ann Hematol 2015; 94:707–9.

- Sun XH, Wang ZY, Yang HY, et al. Clinical, pathological, and genetic analysis of ten patients with MYH9-related disease. Acta Haematol 2013; 129:106–13.
- Yoshimi A, Toya T, Nannya Y, et al. Spectrum of clinical and genetic features of patients with inherited platelet disorder with suspected predisposition to hematological malignancies: a nationwide survey in Japan. Ann Oncol 2016; 27:887–95.
- Zhang S, Zhou X, Liu S, et al. MYH9-related disease: description of a large Chinese pedigree and a survey of reported mutations. Acta Haematol 2014; 132:193–8.

$d_{\text{intron 40}}$.

Table 3

Studies that identified variants in *MYH9* as responsible for non-syndromic deafness. Each variant was identified in a single family.

Study	Investigated cohort	*MYH9* gene variant	MYH9 protein variant	Phenotype inheritance	Phenotypic features of deafness
Wu et al., 2013	12 patients with AD or AR SNHL	c.3766G>A	p.Glu1256Lys	AD	b-SNHL, profound, progressive, mostly in mid and high frequencies
Miyagawa et al., 2013	216 patients with b-SNHL	c.2404C>T	p.Arg802Trp	AD	b-SNHL, moderate, mostly in mid and high frequencies
		c.3016_3017insGAG	p.Thr1006fs	AR	b-SNHL, severe, all frequencies
		c.4352C>T	p.Ala1451Val	AD	nr
Neveling et al., 2013	36 patients with HL	c.2507C>T	p.Pro836Leu	AD	nr
Kim et al., 2016	75 patients with AD non-syndromic HL	c.3909C>A	p.Phe1303Leu	AD	b-SNHL, profound, progressive, mostly in mid and high frequencies
		c.5188C>T	p.Arg1730Cys	AD	b-SNHL, severe, mostly in high frequencies
		c.5353C>T	p.Arg1785Cys	AD	b-SNHL, severe, mostly in mid and high frequencies
Sloan-Heggen et al., 2016	1119 patients with HL	c.4489C>T	p.Arg1497Trp	AD	b-SNHL, mild to moderate

Abbreviations: HL, hearing loss; SNHL, sensorineural hearing loss; AD, autosomal dominant; AR, autosomal recessive; b-, bilateral; nr, not reported.